Master's Thesis

SYNTHESIS OF VISIBLE LIGHT ACTIVE PHOTOCATALYSTS AND THEIR APPLICATION IN PHOTOCATALYTIC DEGRADATION OF ORGANIC COMPOUNDS

Junyoung Jeong

Department of Urban and Environmental Engineering

(Environmental Science and Engineering)

Graduate School of UNIST

2016

SYNTHESIS OF VISIBLE LIGHT ACTIVE PHOTOCATALYSTS AND THEIR APPLICATION IN PHOTOCATALYTIC DEGRADATION OF ORGANIC COMPOUNDS

Junyoung Jeong

Department of Urban and Environmental Engineering
(Environmental Science and Engineering)

Graduate School of UNIST

Synthesis of Visible Light Active Photocatalysts and their Application in Photocatalytic Degradation of Organic Compounds

A thesis
submitted to the Graduate School of UNIST
in partial fulfillment of the
requirements for the degree of
Master of Science

Junyoung Jeong

7. 18. 2016

Approved by

Advisor
Changha Lee

Synthesis of Visible Light Active Photocatalysts and their Application in Photocatalytic Degradation of Organic Compounds

Junyoung Jeong

This certifies that the thesis of Junyoung Jeong is approved.

7. 18. 2016

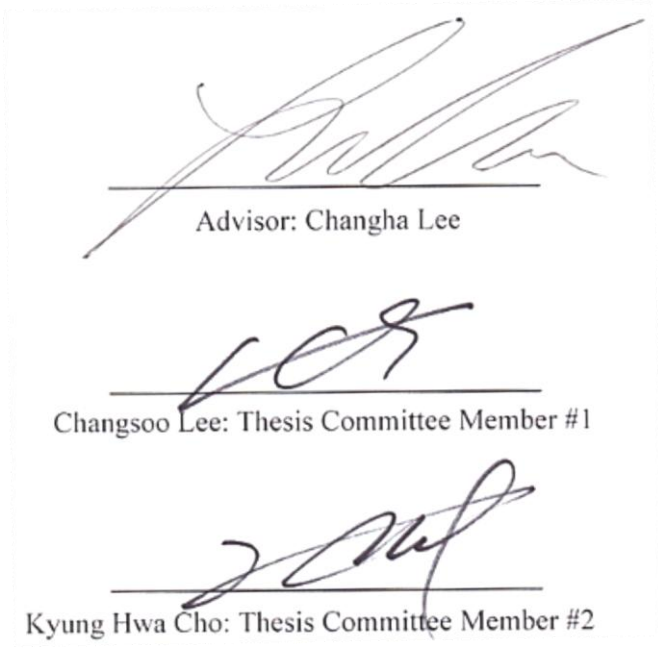

Abstract

Nowadays, the presence of the various noxious compounds in water resources becomes a worldwide sensation in regard with the exploitation of progressive and field-applicable water treatment technology. Titanium dioxide (TiO_2) is the most effective photocatalyst for decomposition of organic contaminants in water resources due to its high photoactivity for the production of hydroxyl radical, low cost, chemical inertness, and low toxicity. However, TiO_2 is only activated by ultraviolet light. Accordingly, many attempts have been made to extend the available range to the visible-light area by metal and non-metal doping, dye photosensitization and so on.

In the first part of study, 2-ethylimidazole-TiO_2 (N-doped TiO_2) photocatalyst was synthesized by a simple method by 2-ethylimidazole as the specific nitrogen source, and its photocatalytic activity was examined for degradation of microcystin-LR under visible light irradiation because harmful cyanobacterial toxins (e.g., microcystins) have raised concerns about the safety of drinking water resources. The synthesized photocatalyst was compared to other N-doped TiO_2 materials reported in previous studies for the photocatalytic activity.

In the second part of study, Co-H_2O_2-TiO_2 can be synthesized using the precursor, TTIP (Titanium Tetraisopropoxide), and hydrogen peroxide. Additionally, the efficiency of H_2O_2-TiO_2 in visible light rage was experimentally confirmed through the previous study. In this study, a simple cobalt doping method was utilized for increasing the photoactivity of H_2O_2-TiO_2. Then, decomposition efficiency was checked by applying various contaminants. Finally, the mechanism of photocatalyst was proposed with an explanatory diagram.

CONTENTS

List of Figures

List of Tables

Chapter 1. Introduction

I. Global trend of research

The laboratory of Honda-Fujishima in the university of Tokyo has conducted the photocatalyst research since the initial study began in 1972 (Fujishima *et al*., 1972). This is a starting point for the photocatalytic material and its application technology research. In addition, the government of Japan has aggressively supported the related research and development of photocatalyst since 2003. Accordingly, photocatalytic companies are more than 1000 of the world photocatalyst market. Especially, the corporations such as Ishihara Industries, Sakai Chemical have an ability to make raw materials for mass production of titanium dioxide nanoparticle. For the practical application, some companies in Japan were the most aggressive around the world. For example, Toto Inc. commercialized the photocatalytic antibacterial tile wall and sound insulation board on the road in 1995. Besides, it is known that the scale of relevant market was more than four million dollars in 2006.

The newly developed photocatalytic technology in Japan, a few examples, Fujitsu in the university of Tokyo has developed titanium dioxide powder regarding replacement of some calcium apatite with titanium. Then, this technology, which showed excellent adsorption and disinfection performance against the bacteria, was relocated to the Daikin co. for commercialization. In conclusion, the lively researches have consistently conducted until now. In addition, Asahi of Toyota Central R&D Center developed visible response photocatalytic titanium dioxide coated ceramic and nitrogen by using reactive sputtering method. Also, AIST (Agency of Industrial Science and Technology) synthesized visible response photocatalyst powder, hydroxyapatite-coated photocatalyst powder and a filter attached to these photocatalytic powders on the surface of the high-strength silicon body. Moreover, Miao in Nagoya Institute of Technology reported excellent investigation through the antibacterial experiments of ceramic coated titanium dioxide by sputtering it. It shows the efficiency of sterile 93% under 400 uW/cm^2 of ultraviolet for 2 hours. As mentioned, the results regarding materials and various applications in Japan can be described as the best in the world.

On the other hand, the research in United States and Europe was mainly conducted for applications in the field of water treatment. Recently, they headed the research in regard with small stream pollution purification, industrial wastewater treatment. However, the most of researches didn't commercialize in general because they couldn't show innovative results involved the chronic problem of photocatalyst.

In the South Korea, the recent trend of photocatalyst technology has been widely published in regard with usage for solving a sick building syndrome by photocatalyst. As mentioned in the various

papers, the reaction rate of photocatalyst was described as slow and low efficiency that the decomposition rate of contaminants would decrease gradually. In addition, it is difficult to select the wanted target compounds and to react without the irradiation of ultraviolet rays. In the domestic of South Korea, many research groups have been performed to get over these problems (Cho *et al*., 2005). Also, a lot of big and small businesses in South Korea are conducting a joint study with the related laboratories. However, technical improvement still has not arrived to advanced technology in the world. The performance of them has not been normalized and standardized yet.

However, the research group in South Korea is currently performing photocatalyst study in conglomerate and national institute such as Korea Research Institute of Chemical Technology, Institute of Industrial Science, Institute of Energy Research, Samsung Electronics, and LG Electronics and so on. The major research groups currently interest in the production the photocatalyst nanoparticle and manufacturing composite in regard with photocatalyst. In addition, the photocatalyst researches for immobilization by using a glass, polymers, metals, ceramics, paper and fiber were applied to photolysis of various organic substances and wastewater treatment. Additionally, the photocatalyst researches for antibacterial, air freshener, deodorant are being accelerated in recent years. Table 1 shows domestic market scale of photocatalyst based on the report of Korean government.

Table 1. Domestic market scale of photocatalyst (unit: million dollars, Source: Ministry of Trade, Industry and Energy in Korea)

	2005 year	2005 year	2010 year
Environmental services	38.98	78.85	136.39
Environmental resources industry	28.38	62.77	118.54
Environmental facility	22.61	46.35	62.62
Total	89.97	187.97	317.55
Market of photocatalyst		3.76	25.00
Portion in environment market		2%	8%

II. Definition of Photocatalyst

The catalyst was defined as the substances which show the improvement of the effect and response time. In reality, the word of photocatalyst could be a little strange but it is compound with photo and catalysts activated by using light. That is, it means a material to cause a catalytic reaction by taking advantage of the light. In fact, there are lots of photocatalyst around our circumstance and it can be common in the environment. The plants that exist on Earth convert the water and carbon dioxide to oxygen and complex carbohydrates. In these procedures, the most important reaction was fulfilled by typical photocatalyst called chlorophyll. Terrestrial living organisms are breathing through oxygen made by photosynthesis of chlorophyll. In other words, if there is no photocatalyst chlorophyll, all living things will not be present inevitably. Solar energy is seriously associated with survival in all plants and animals as well as humans. The important factor is the light wavelength and particle mass described energy at the same time. It has the unique and complex characters. The corpuscular of light was belonged to the electromagnetic waves and steady energy. In reality, the energy of the photon would shift by depending on the specific wavelength. The shorter the wavelength is, the stronger the energy would be. In addition, the solar light is shown as white light but it is a mixture of different wavelengths of light. The visible light for eyes of human has the range between 400 nm and 800 nm. When the light was less than 400 nm, it called ultraviolet light. Infrared light contained the wavelength over 800 nm. The visible light range, in the vicinity of 450 nm, it can be seen that the maximum energy of light. In our future, if utilizing the energy of lights very well, it would mean that it may also be used effectively in the range of 400 nm to 450 nm (Gerischer *et al*., 1992). The energy of the light is measured by analyzing the wavelength and frequency. The units of wavelength usually expressed as nanometers (nm) that it is the one billion cycles per second. The UV light normally has a shorter wavelength than the visible light (400 nm). In addition, the ultraviolet light can be divided into each of wavelengths depended on the range of UV-A (320 nm - 400 nm), UV-B (290 nm - 320 nm), UV-C (200 - 290 nm). Likewise, the visible light has the unique colors in accordance with the different wavelength. It was consisted of the red (610 - 700 nm), orange (590 - 610 nm), yellow (570 - 590 nm), green (500 - 570 nm), blue (450 - 500 nm), purple (400 - 450 nm). Also, general natures of the light have a reflection, refraction, synthesis, distribution and strong straightness. Even though the energy of light from starting the Sun has more than 10,000 times than fossil energy like oil or coal, the utilization of it would stay in a small part as ever.

III. Theoretical background of Photocatalyst

Typical crystal structures of TiO_2 may be distinguished into three kinds such as anatase, rutile and brookite (Reyes-Coronado *et al*., 1992). Even though stable crystal phase is rutile structure thermodynamically, anatase is easily obtained in the production of TiO_2. If processed approximately 700 celsius degrees or more high-temperature, this crystalline phase has various characteristics in the stable rutile. The crystal phases of anatase and rutile are between 3.0 eV and 3.2 eV called the band gap energy. The crystal phase of rutile could absorb wider ultraviolet region of the light when comparing to crystalline phase of anatase. When using same light source, it is expected to show a higher luminous efficiency. However, these results were not proved obviously regarding the exact mechanism. It is only expected that's why anatase crystal structure has high oxygen adsorption capacity. Also, it is estimated that the pace of the recombination rate constant in regard with the generated electrons and holes by the light would be faster in the rutile crystalline phase. In addition, there is a case of the mixed-crystal structure contained the anatase and rutile. In that case, it stands out rather than single anatase crystal structure or rutile crystal structure. Accordingly, the decrease of rutile surface area about the enhancement of the particle size would be additional reason because the rutile crystallization can be created under the high temperatures condition. In addition, there are a number of all kinds of photocatalyst such as Cds, ZnO and TiO_2. Each a photocatalyst has optical excitation response (photo-excitation) separately. That is, the needed energy for photocatalyst activation is necessarily different by the light irradiation. Some materials and its band gap energy for the photocatalyst activation are as shown in Table 2. To take advantage of the TiO_2 anatase crystals, the wavelength (387.5 nm) of the light is needed for occurring photo-excitation reaction. This wavelength value could be calculated by using some formula related light and its wavelength.

TiO_2 is a kind of photocatalyst as a light semiconductor which made little electricity under irradiation condition (Hoffmann *et al*., 1995). In general, the difference between a semiconductor and an optical semiconductor is as follows. In the case of a semiconductor, to generate a current flow, the electrons in the valence band have to go to the conduction band. However, the electrons in the optical semiconductor can jump to the conduction band when having a significant light energy in the band gap which means the valence band and conduction band.

OH radical's generation mechanism of the photocatalyst can be described that it starts the step of generating pairs of the hole (h^+) and electron (e^-) in the photocatalytic particles by the light (wavelength < 390 nm) (Linsebigler *et al*., 1995). The h^+_{VB} is the positive hole in the valence band (VB) and e^-_{CB} is an electron on the conduction band (CB). The generated hole in the surface of the TiO_2 forms OH radicals by combining the hydroxide ions and the water molecules. It is made the oxidation with the water molecules of hole (h^+) on the valence band (2.1, 2.2, 2.3). The emitted

electrons react with oxygen or hydrogen peroxide as the acceptor of electrons in the water. At this time, the oxygen or electron acceptor in the surface of TiO_2 would be reduced and the electrons on the conduction band make superoxide ion (O_2^-) as being accepting oxygen molecules (2.4). The formed superoxide ions also reproduce OH and O_2 by combining with water molecules (2.5, 2.6). The adsorbed organic material on the TiO_2 surface oxidizes directly or is oxidized by the formed OH radicals. Figure 1 shows the simple diagram for main mechanism of titanium dioxide briefly.

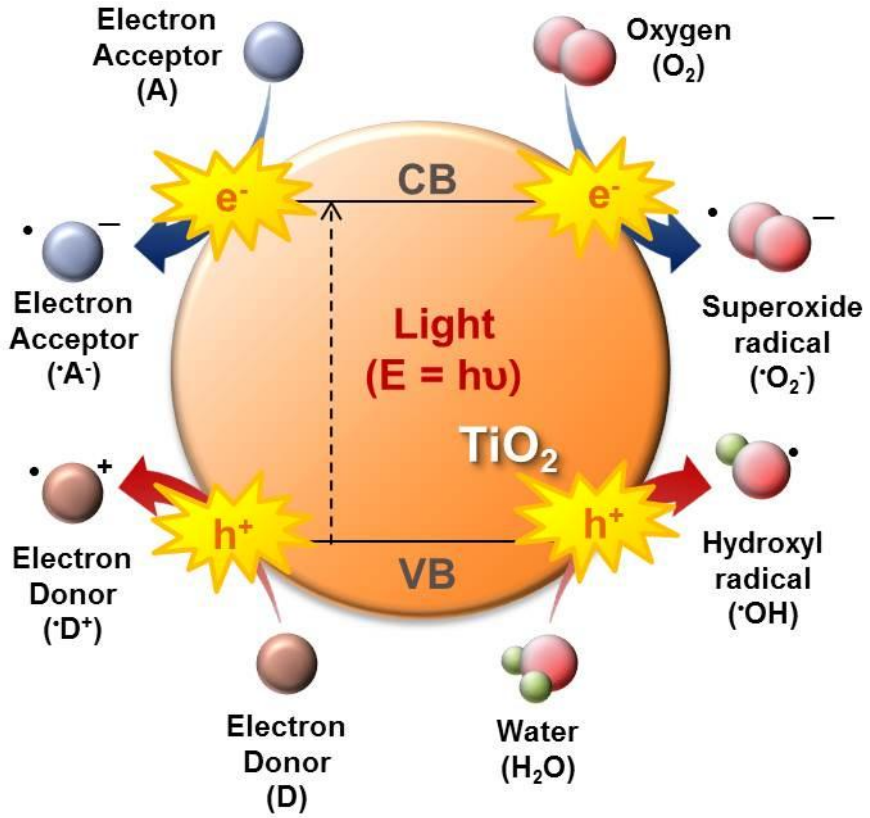

Figure 1. The diagram for main mechanism of titanium dioxide (TiO_2)

Plus, the reaction of the photocatalyst can be divided in accordance with the presence or absence of water. When the aqueous solution is not present, the generated amount and the rate of electrons and the hole is related with the position, the type and intensity of the light source, catalysts and concentration etc. In addition, the reactions of the electrons and holes with the reactants are influenced by the pH and temperature sensitively. However, H_2O on the positive solution acts to neutralize the hole and form OH radicals. Thus, the generated $^{\bullet}OH$ could degrade almost all targets because it has a substantial high redox potential to oxidize something. If the electrons do not have a place where can be recombined with the holes, it forms O_2^- due to the electronic transition on the surface of the adsorbed O_2. Then, it performs the formation of H_2O_2 to react H_2O on the surface. In the same manner,

this H_2O_2 plays a role as the strong oxidation agent. The generated H_2O_2 and OH radical like previous explanation decompose the harmful organic substances into harmless CO_2 and H_2O (Wu *et al*., 1999).

$$TiO_2 + hv \rightarrow TiO_2 (h^+_{VB} + e^-_{CB}) \quad (2.1)$$

$$TiO_2 (h^+_{VB}) + H_2O \rightarrow TiO_2 + OH^- + H^+ \quad (2.2)$$

$$TiO_2 (h^+_{VB}) + OH^- \rightarrow TiO_2 + {}^{\bullet}OH \quad (2.3)$$

$$TiO_2 (e^-_{CB}) + O_2 + H^+ \rightarrow TiO_2 + HO_2^{\bullet} \rightarrow O_2^{\bullet -} + H^+ \quad (2.4)$$

$$TiO_2 (e^-_{CB}) + HO_2^{\bullet} + H^+ \rightarrow H_2O_2 \quad (2.5)$$

$$TiO_2 (e^-_{CB}) + H_2O_2 \rightarrow TiO_2 + OH^- + {}^{\bullet}OH \quad (2.6)$$

Table 2. Band gap energy of each phtocatalyst

Photocatalyst	Band gap energy (eV)
TiO_2	3.2
GaP	2.2
ZrO_2	2.2
Si	1.1
CdS	2.5
ZnO	3.2
Fe_2O_3	2.2
WO_3	2.5
SnO_3	3.5

IV. Objectives of the study

The present research had the following two specific objectives:

1. To synthesize and characterize the visible light active TiO_2 photocatalysts by a facile treatment using a 2-ethylimidazole. The potential of the synthesized materials was assessed for the oxidation of organic contaminants in water resources under visible light irradiation condition.

For this purpose, TiO_2 (Degussa P25) and 2-ethylimidazole were synthesized as newly modified visible response photocatalyst, and the removal of microcystin-LR was studied with reaction rate constant and the effectiveness of degradation. Also, the oxidation of total residual compounds was investigated after all reaction.

2. To synthesize and characterize the better visible light response H_2O_2-TiO_2 by a facile treatment using a sol-gel method for doping of metal ion. The effectiveness of the synthesized materials was evaluated for the oxidation of organic compounds in water resources under visible light irradiation condition.

The primary objectives of this study were to evaluate the removal efficiency of organic compounds by new cobalt doped H_2O_2-TiO_2. For this purpose, the removal of 4-chlorophenol was examined during visible irradiation with various factors affecting the efficiency, which would provide insight into assessing the strategies for evaluating the modified photocatalysts. In addition, the formation of HCHO or 4-HBA in the reaction is investigated for explanation with regard to mechanism of cobalt doped H_2O_2-TiO_2 (Wang *et al*., 2004).

Chapter 2. Materials and Methods

I. Synthesis of 2-ethylimidazole-TiO_2

All chemical reagents, TiO_2 (Degussa P25, Germany), $C_5H_8N_2$ (2-Ethylimidazole 98% Sigma-Aldrich, USA), were used without more purification. First, 2-Ethylimidazole was added into 10 mL of deionized water (18 MΩ·cm Milli-Q water from a Millipore system) containing commercial TiO_2 (Degussa P25, Germany) under vigorous stirring on the plate (6-Position Multi-Stirrer/Hot plate Dai-han SMHS-6, Republic of Korea). Then, the solvent was evaporated at 50 ℃ for several hours while stirring. The white powder was obtained following dry procedure. The precipitates were calcined at 350 ℃ in the Chamber Furnace (Digital Muffle Furnace Dai-han FH-12, Republic of Korea) for 3 hours after making N_2 condition. As a result, yellowish N-doped TiO_2 photocatalyst was finally obtained. If finished to burn, take out powder from furnace immediately for cooling at the room temperature (22 ± 2 ℃). The taken sample was filtered by 0.45 μm with deionized water. The photocatalytic activity was optimized when the mass ratio of TiO_2 to 2-ethylimidazole was 1:8 wt. %. The same method was used to set optimal portion of 2-ethylimidazole quantity.

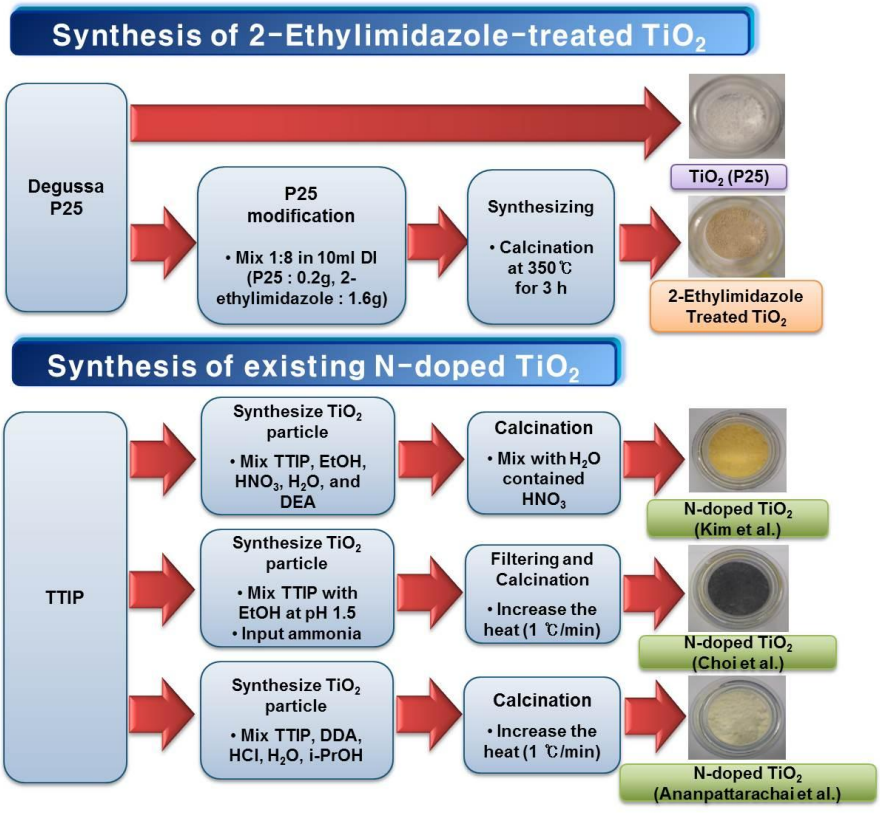

Figure 2. The diagram about fabrication process of nitrogen doped titanium dioxide

II. Synthesis of Cobalt doped H_2O_2-TiO_2

$Ti[OCH(CH_3)_2]_4$ (Titanium(IV) Tetraisopropoxide 97% Sigma-Aldrich, USA), H_2O_2 (30% (v/w) stock solution Sigma-Aldrich, USA), Cobalt(II) nitrate hexahydrate (ACS reagent 98% Sigma-Aldrich, USA), C_2H_5OH (200 Proof, Sigma-Aldrich, USA) and Nitric acid (ACS reagent 98% Sigma-Aldrich, USA) were utilized with no further purification. As previous studies, H_2O_2-TiO_2 was synthesized by sol–gel preparation method. TTIP solution (2 mL) was added to 1 M of hydrogen peroxide solution (10 mL) with stirring for 1 h. The resulting powder was collected by centrifugation (3000 rpm) for 15 min and washed three times with deionized water (50 mL). Then, this powder was dried at 50 ℃ for 4 h. In this study, H_2O_2-TiO_2 was additionally modified for enhancement of reusability and visible response as the facile doping methods. Likewise, Co-H_2O_2-TiO_2 can be synthesized using the precursor, TTIP (Titanium(IV) Tetraisopropoxide) of TiO_2. The detailed procedure was as follows: $Ti[OCH(CH_3)_2]_4$ (1.25 mL) was dissolved in 25 mL C_2H_5OH (solution 1) by dropwise. Then, 250 mL of Hydrogen peroxide (1 M) and Cobalt nitrate (0.2 M) adjusted pH 1.5 with nitric acid (solution 2) was prepared. Solution 1 was dropwised to solution 2 with busy stirring. The mixed solution would stir overnight vigorously and was heated to 50 ℃ on the hot plate. Finally, pure and light-yellowish powder of Cobalt doped H_2O_2-TiO_2 obtained. It was washed by DI water and then dried in the arid oven. The concentration of H_2O_2 (1 M) was optimized in the previous study. So, the optimization point of cobalt's concentration was suggested after experiments for comparison with various portions by degrading organic pollutants.

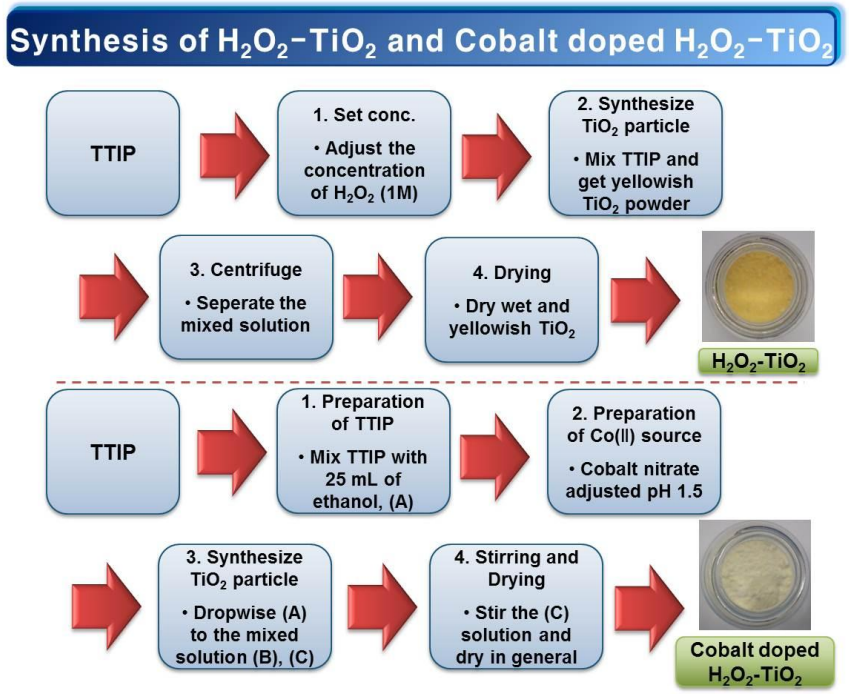

Figure 3. The diagram in regard with main process of fabrication of modified H_2O_2-TiO_2

III. Experimental methods

Photoactivity Test. Photoactivity experiment was performed in 50 mL cylindrical quartz reactor at room temperature. The 0.5 g/L photocatalyst nanoparticle was located in the circular quartz cell reactor. Then, TiO_2 nanoparticles, which dispersed in water by sonication for 5 min, were transferred to a quartz reactor containing organic pollutants. In the case of harmful cyanobacterial toxins (e.g., microcystins), the solution pH was adjusted at 7.0 for making neutral water condition. The reactor was initiated upon different types of light irradiation by 150 W Xenon and 4 W Fluorescence lamp mounted with a UV block filter that cut off particular light wavelength (320 - 400 nm). The initial conditions of various contaminants were as follows: Phenol, 4-Chlorophenol, Acetaminophen, Benzoic acid and Carbamazepine were 10 uM. Initial concentration of microcystin-LR was 100 ppb of World Health Organization's standard. Generally, the sampling was repeatedly fulfilled 8 times by using 1 mL syringe in accordance with overall reaction time.

Characterization. After synthesis of separate photocatalyst by sol-gel methods, the material was characterized by many spectroscopic analysis methods. X-ray diffraction (XRD) pattern on the materials was analyzed to ensure structural properties by D8 Advance II X-Ray diffractometer (Germany, Bruker) crystallographically with Cu Kα radiation in the wavelength 1.5406 Å. Additionally, it was fulfilled from 10^{o} to 80^{o} (2θ) as the analysis with the step size (0.05^{o}) and the step time of 3 seconds to detect the crystallinity. UV-Vis absorption spectra data was utilized for the analysis of UV-Vis near-infrared (NIR) on Cary 5000 scan from 200 to 800 nm. X-ray photoelectron spectroscopy (XPS) measurements, which were utilized to check the chemical element concerning the dopant. Transmission electron microscopy (TEM) analysis was fulfilled with JEOL JEM-2100F which operated at 200 kV. TEM image was got ready on the carbon coated Formvar copper grid and was conducted under the room temperature condition for several hours. Fourier transform infrared spectroscopy (FT-IR) of separate photocatalyst was obtained using Varian 670 FT-IR spectrometer. Additionally, FT-IR spectra data was analyzed by multi-reflecting IR beams and under 4000 - 400 cm^{-1} of special range using a MCT detector.

IV. Analytical methods

C_6H_5OH (Phenol 99.5% Sigma-Aldrich, USA), C_6H_5ClO (4-Chlorophenol 99.0% Sigma-Aldrich, USA), $C_{49}H_{74}N_{10}O_{12}$ (Microcystin-LR ALX-350-012 95% Enzo Life Sciences), HCHO (Formaldehyde solution 37 wt. % in H_2O Sigma-Aldrich, USA), $C_7H_9ClN_2O_2$ (4-Hydrazinobenzoic acid hydrochloride 98% Sigma-Aldrich, USA), $C_{17}H_{17}NO_6$ (Acetaminophen 99.0% Sigma-Aldrich, USA), $C_7H_6O_2$ (Benzoic acid 99.5% Sigma-Aldrich, USA), $C_{15}H_{12}N_2O$ (Carbamazepine powder Sigma-Aldrich, USA) and $C_{15}H_{16}O_2$ (Bisphenol-A 99% Sigma-Aldrich, USA) were dissolved in deionized water for making respective solutions.

Main target, 4-chlorophenol was analyzed by ultra-performance liquid chromatography (UPLC; Dionex SR 3000, Thermo Fisher Scientific Inc., USA) with UV detection at 230 nm. The separation was performed on Agilent Eclipse XRD-C18 column (150 mm × 4.6 mm, 3.5 μm) using 0.1% aqueous solution of the phosphoric acid and acetonitrile as the ratio of 6 : 4. It flows in 1.5 mL/min. Also, a variety of targets which excepted for 4-Chlorophenol were analyzed by using a high-performance liquid chromatography (HPLC; Dionex Ultimate 3000, Thermo Fisher Scientific Inc., USA) with reference database regarding condition of analysis by high performance liquid chromatography as shown below Table 3 to 5. Also, the titanium sulfate method was used to measure the concentration of hydrogen peroxide (ε_{405} = 730 $M^{-1}s^{-1}$; Eisenberg, 1943).

Table 3. Condition of analysis by high-performance liquid chromatography

Oxidants	Phenol	4-Chlorophenol	Microcystin-LR
Flow rate	1.0 mL/min	1.5 mL/min	1.5 mL/min
Eluent	0.1% phosphoric acid: 50% Acetonitrile: 50%	0.1% phosphoric acid: 60% Acetonitrile: 40%	0.1% phosphoric acid: 50% Acetonitrile: 50%
Run time	3.5 min	4.0 min	4.0 min
Detection λ	277 nm	230 nm	227 nm
Injection volume	50 μL	50 μL	50 μL
Oxidants	HCHO	4-HBA	Acetaminophen
Flow rate	1.0 mL/min	1.0 mL/min	1.5 mL/min
Eluent	0.1% phosphoric acid: 50% Acetonitrile: 50%	0.1% phosphoric acid: 80% Acetonitrile: 20%	0.1% phosphoric acid: 90% Acetonitrile: 10%
Run time	6.0 min	10.0 min	3.0 min
Detection λ	350 nm	270 nm	241 nm

Injection volume	50 μL	50 μL	50 μL
Oxidants	Benzoic acid	Carbamazepine	Bisphenol A (BPA)
Flow rate	1.0 mL/min	1.5 mL/min	1.0 mL/min
Eluent	0.1% phosphoric acid: 50% Acetonitrile: 50%	0.1% phosphoric acid: 60% Acetonitrile: 30% Methanol: 10%	0.1% phosphoric acid: 55% Acetonitrile: 45%
Run time	4.0 min	5.0 min	7.0 min
Detection λ	227 nm	215 nm (285 nm)	230 nm
Injection volume	50 μL	50 μL	50 μL

Chapter 3. Results and Discussion

I. Synthesis of 2-ethylimidazole-TiO_2 and its application in visible light response photocatalysis of microcystin-LR

1.1. Optimization of material

First of all, 2-ethylimidazole treated TiO_2 was optimized by experimenting the degradation of 4-chlorophenol. Actually, there were the necessary three factors for optimization such as temperature of calcination, material mixing ratio and gas condition for calcination (nitrogen gas or oxygen gas). Figure 4 shows the comparison of the efficiency regarding 4-chlorophenol's degradation for four hours. When the ratio of bare TiO_2 (Degussa P25) and 2-ethylimidazole was 1:8 wt. %, this material had the best processing efficiency. So, afterwards, the ratio of one/eight was lastly chosen for fabricating additional 2-ethylimidazole-TiO_2.

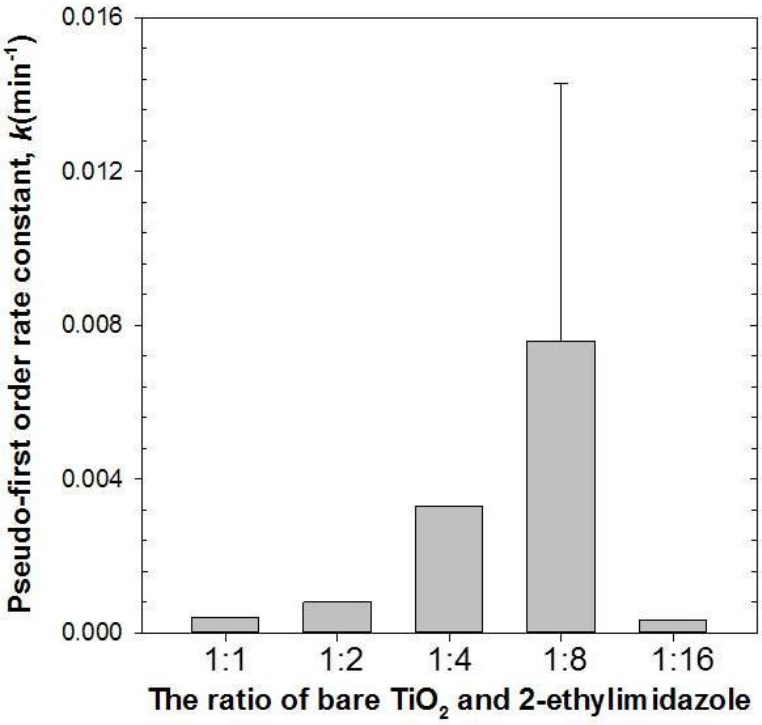

Figure 4. The comparison of the degradation efficiency in accordance with different ratio of TiO_2 (P25) and 2-ethylimidazole-TiO_2 under the visible light (>400 nm)

$[TiO_2]_0$ = 0.5 g/L; $[4\text{-chlorophenol}]_0$ = 10 μM; [Fluorescent lamp : 6 ea]; [Reaction time : 4 h]

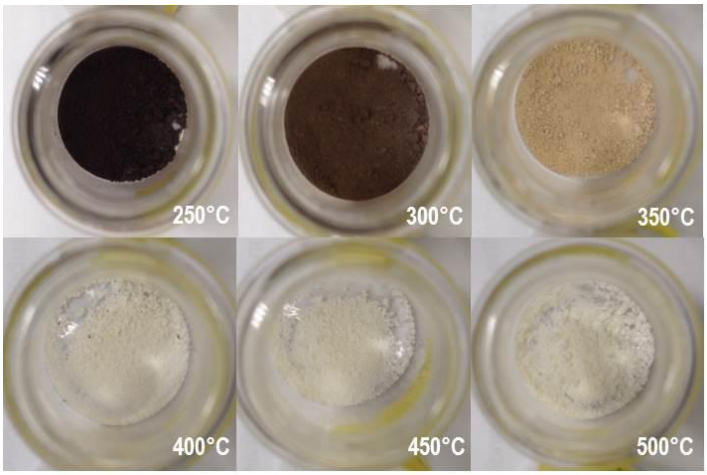

Figure 5. Different colors 2-ethylimidazole-TiO_2 in accordance with various sintering temperatures

Secondly, this materials also shows different colors related its efficiency (Bacsa *et al*., 2005). Figure 5 explained the colors in accordance with various sintering temperature. As exposed, sintering temperatures were set at 50 ℃ intervals. Like a figure, the higher the sintering temperature was, the brighter the color of the material was. When the temperature of calcination was below 300 ℃, the colors of this material would be darker. In addition, the color of photocatalyst is very important because the acceptance capacity of light is deeply related to its exposed colors. The newly set 2-ethlimidazole-TiO_2 was tested by degrading the 4-chlorophenol as before.

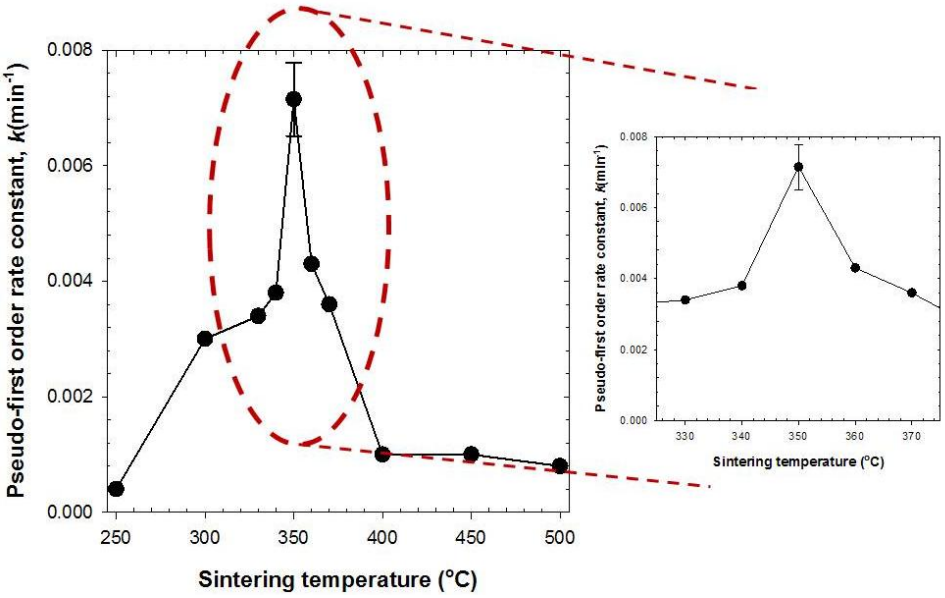

Figure 6. The efficiency of 2-ethylimidazole-TiO_2 fabricated under different sintering temperatures (>400 nm)

$[TiO_2]_0$ = 0.5 g/L; [4-chlorophenol]$_0$ = 10 μM; [Fluorescent lamp : 6 ea]; [Reaction time : 4 h]

Figure 6 shows pseudo-first order rate constant, *k* value (min^{-1}) of 2-ethylimidazole-TiO_2 for finding out the optimization point with regard to sintering temperature. As the red dotted line means, when temperature of calcination was set at 350 ℃, it decomposed target compound very well. In the same vein, 350 ℃ was finally chosen for the best efficiency.

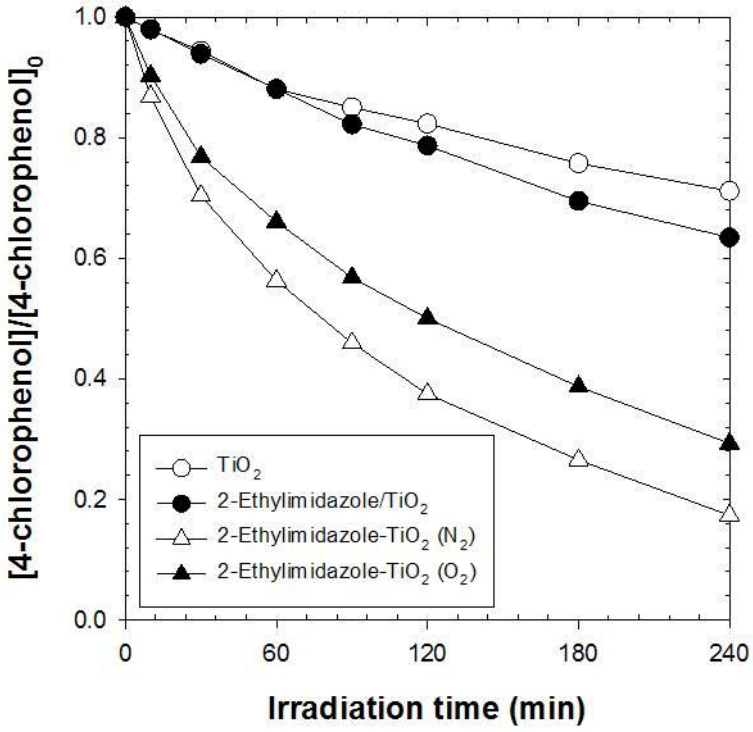

Figure 7. The comparison of the degradation efficiency of 2-ethylimidazole-TiO_2 fabricated under different gas condition (>400 nm)

$[TiO_2]_0$ = 0.5 g/L; $[4\text{-chlorophenol}]_0$ = 10 μM; [Fluorescent lamp : 6 ea]; [Reaction time : 4 h]

Thirdly, the gas condition of calcination is one of the most important factors for optimization because of accelerating some chemical activity. As shown in Figure 7, 2-ethylimidazole solution composed TiO_2 was also experimented for suggestion of control status. The nitrogen gas and oxygen gas were fully utilized by being injected to the furnace through the gas line in the laboratory. If comparing with the nitrogen gas and oxygen gas in the graph, when the gas condition was the nitrogen, it showed the best efficiency. As mentioned later on the characterization of material, this data implies that the nitrogen gas assisted to take doping of nitrogen element.

In summary, the ratio of bare TiO_2 (Degussa P25) and 2-ethylimidazole (one/eight), 350 ℃ for calcination and the nitrogen gas condition were finally selected as based on upper data.

1.2. Characterization of material

In Figure 8, X-ray diffraction spectral analysis and the result of analysis data are provided (Wang *et al*., 2009). The presence of anatase phase is observed for 2-ethylimidazole treated TiO_2 which calcinated at 350 ℃. The anatase phase of titanium dioxide has generally been explained with no phase modification to rutile after rising the calcination temperature over 500 ℃. Also, it can be interpreted from the XRD patterns that 2-ethylimidazole treated TiO_2 shows broad peaks which indicate the formation of nanoparticles when compared to bare TiO_2 (Degussa P25). The general crystallization can be explained that an agglomeration of particles at high temperatures was caused by the increase of calcination temperature and the particle size.

The crystalline phase of bare TiO_2 and 2-ethylimidazole treated TiO_2 could not be changed as shown a complete anatase phase in Figure 8. When comparing with bare TiO_2 and 2-ethylimidazole-TiO_2, a brand-new one would possess the tinier crystallite size. It is regarded that nitrogen doping of this material could expand the anatase crystallization. It loosens the amorphous titania transformation to anatase species due to the lower crystallinity of 2-ethylimidazole-TiO_2.

The pore volume of 2-ethylimidazole-TiO_2 could be expected approximately several times greater than it of bare TiO_2. This being so, 2-ethylimidazole treated TiO_2 would have highly improved BET surface area value. The bigger pore size and tinier crystallinity certainly cause a lot more surface area, which is possible to enhance the photocatalytic activity.

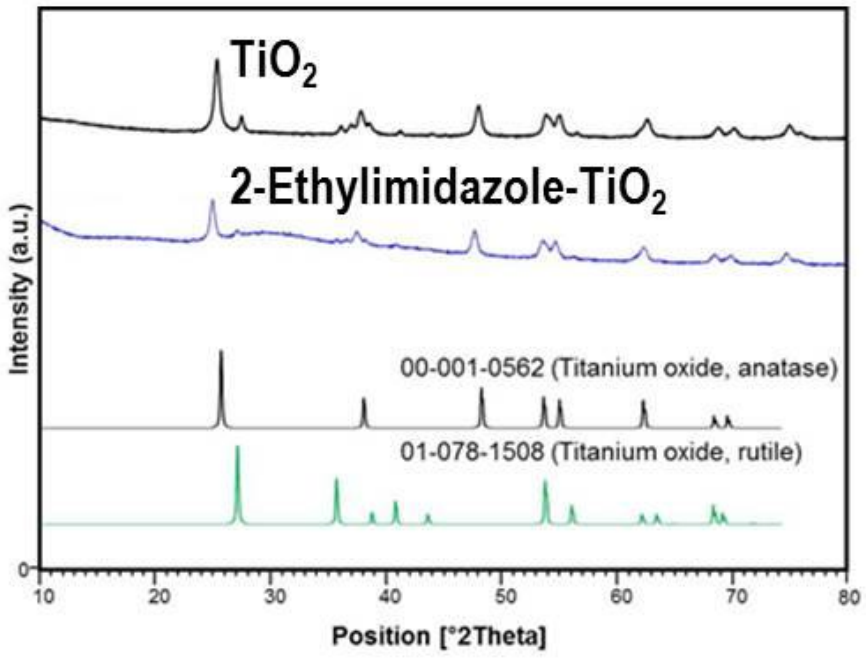

Figure 8. X-ray diffraction pattern of TiO_2 (P25) and 2-ethylimidazole-TiO_2

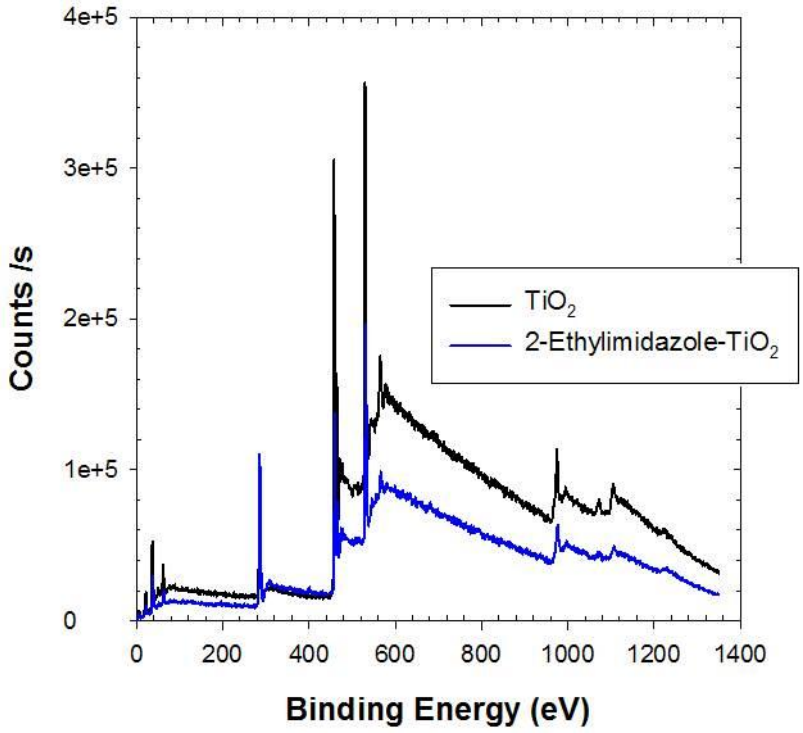

Figure 9. XPS spectra of TiO_2 (P25) and 2-ethylimidazole-TiO_2

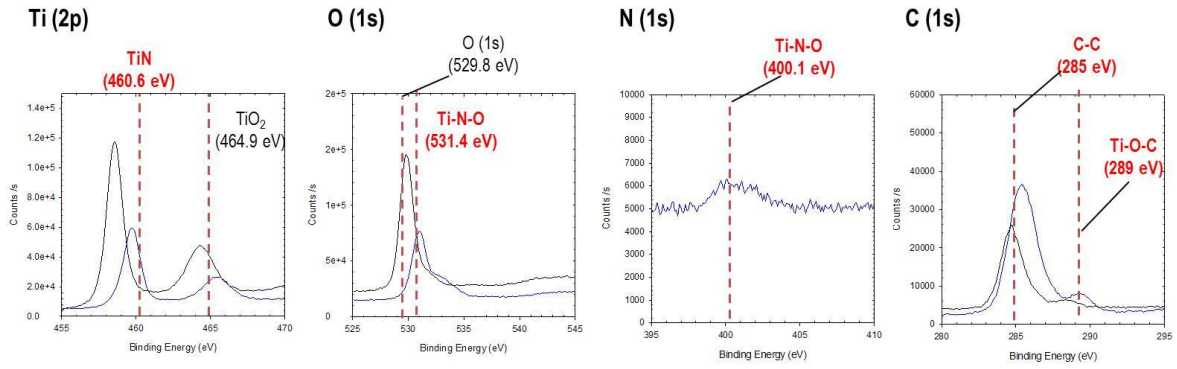

Figure 10. XPS spectra of Ti (2p), O (1s), N (1s) and C (1s) for TiO_2 (P25) and 2-ethylimidazole-TiO_2

To demonstrate the content of Ti and N, XPS analysis on the optimized 2-ethylimidazole-TiO_2 was carried out. As shown in Figure 9 and 10, it shows X-ray photoelectron spectroscopy of Ti 2p, O 1s, N 1s and C 1s (Ohno *et al*., 2003). In general, the preparation methods and conditions largely influence nitrogen XPS spectral features. In addition, the impure nitride also affects the specific position shift of the cognizable doping peak. Hence, the meaning of XPS peaks of N 1s could have sometimes been under the hot argument. However, it is naturally regarded that the specific position was located in the range of 395 - 405 eV. Accordingly, the special peak mainly would be showed in

the vicinity of 400 eV (400.1 eV). According to previous study (Sathish *et al*., 2003), the emergence of the peak over 397 eV could mean that Ti-O-N combinations could have been generated in the nanomaterial. In addition, the density of the electrons about nitrogen atoms could be decreased because of the existence of oxygen atoms. That's why the core level in regard with Ti-N-O shifts higher than it of Ti-N linkages (531.4 eV). That is, the adequate amounts of nitrogen sources were supplied by adding a 2-ethylimidazole. Also, the similar conclusion could be obtained from Ti 2p binding energy area. The specific peaks at 458.5 eV and 462.9 eV are respectively considered as Ti 2p 3/2 and Ti 2p 1/2 in TiO_2 photocatalyst. If compared to the binding energy of bare TiO_2 (460.6 and 464.9 eV), there is approximately 1.1 eV shift toward higher energy, which implies that the interaction of electrons in nitrogen doped TiO_2 is certainly discriminative. This could propose that TiO_2 lattices were modified by nitrogen sources owing to the cooperative manner by nitrogen doping to gather the electrons regarding Ti-O-N. Thereby, the binding energy would be grown-up seemingly. The nitrogen content in 2-ethylimidazole-TiO_2 was determined on 2.67% by the data involved the particular element content (%) on the surface as shown in Table 4.

Table 4. XPS analysis of TiO_2 (P25) and 2-ethylimidazole-TiO_2

Material	C (%)	N (%)	O (%)	Ti (%)	O/Ti (%)
TiO_2 (P25)	30.63	-	48.81	20.08	2.43
2-ethylimidazole-TiO_2	56.76	2.67	3333.91	9.62	3.21

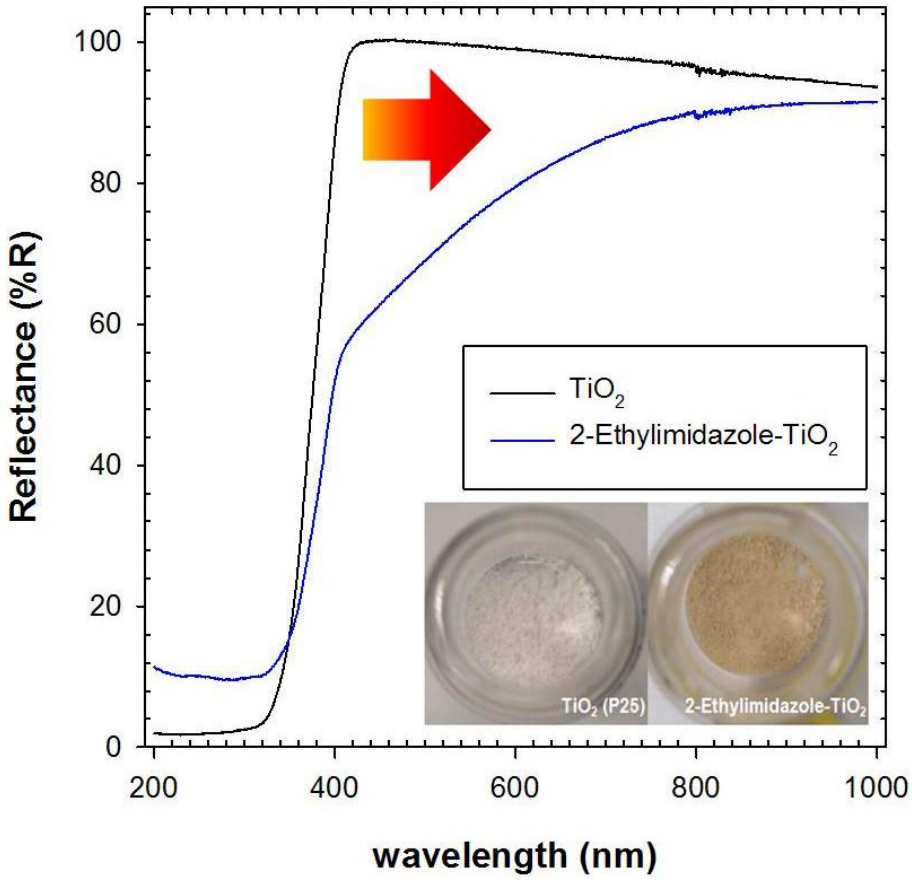

Figure 11. Diffuse reflectance spectra of TiO_2 (P25) and 2-ethylimidazole-TiO_2

In Figure 11, N-TiO_2 correlated an enhanced absorption in the visible light area (400 - 800 nm). The fact could mean the increment of visible light absorption capacity. Accordingly, the band gap energy was detected to close the wavelength in contrast to bare TiO_2, which is obtained with XPS data that the total chemical circumstances are changed a little bit by making an addition of the nitrogen sources. It could demonstrate that the visible light response of 2-ethylimidazole-TiO_2 in this study emerged not only from the internal band gap status, but also through the narrowed band gap energy. In Table 5, there are calculated band gap energies of bare TiO_2 (Degussa P25) and 2-ethylimidazole-TiO_2. As shown below, original control TiO_2 has 3.45 eV value as band gap energy before modification of TiO_2 and 2-ethylmidazole-TiO_2 means exactly narrowed band gap at 3.17 eV value (Morikawa *et al*., 2001). It is the most fundamental reason of having visible light response after modification of original one.

Table 5. Calculated band gap energy of TiO_2 (P25) and 2-ethylimidazole-TiO_2

	Pure TiO_2 (P25)	2-Ethylimidazole-TiO_2
Band gap energy	3.45 eV	3.17 eV

TEM analysis of 2-ethylimidazole-TiO_2 and bare TiO_2 are shown in Figure 12. If compared to the flocculated pure TiO_2, 2-ethylimidazole-TiO_2 is spherical on the uneven division of nanoparticle. The summary shows that the union of nitrogen sources might restrict the agglomeration of particles (Jagadale *et al*., 2003). Additionally, photocatalysts could be usually located in instability due to large surface area. Thus, it easily tends to agglomerate for getting the steady state. In other words, 2-ethylimidazole-TiO_2 nanoparticles will spend a large of energy during the fabrication procedures. This being so, the surface energy in regard with the particle gathering phenomenon would be less than the control TiO_2. 2-ethylimidazole-TiO_2 nanoparticles prolong the crystallization of anatase and retard the change to the anatase phase.

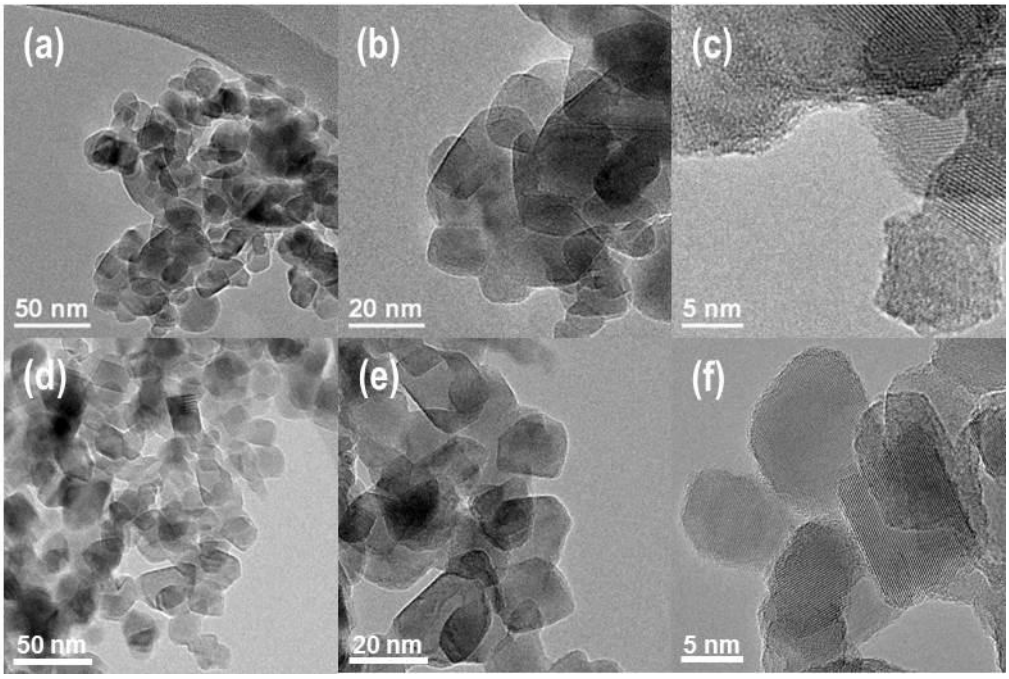

Figure 12. TEM images of 50 nm (a), 20 nm (b) and 5 nm (c) of 2-ethylimidazole-TiO_2 and 50 nm (d), 20 nm (e) and 5 nm (f) of TiO_2 (P25)

1.3. Processing efficiency evaluation

To demonstrate the photocatalytic activity, degradation of 4-chlorophenol as the target compound was investigated with artificial visible light condition with cut-off light filter (>400 nm). As shown in Figure 13, when comparing with pure TiO_2, 2-ethylimidazole-TiO_2 could be expected that the direct illumination with cut-off light filter could lead to show around 80% degradation of 4-chlorophenol during 240 min, which demonstrates the photosensitized capability in regard with 4-chlorophenol molecules by using a high performance liquid chromatography. The photocatalytic response of 2-ethylimidazole-TiO_2 was greatly enhanced under visible light irradiation condition as comparison of the references. Additionally, its data could suggest that the nitrogen doping method had a clear influence on the photocatalytic response regarding modified TiO_2 sample. This material could also degrade perfectly 4-chlorophenol (10 uM) for four and half hours. It shows the perfect decomposition efficiency just for 1 hour under the Xenon lamp condition meant one sun condition.

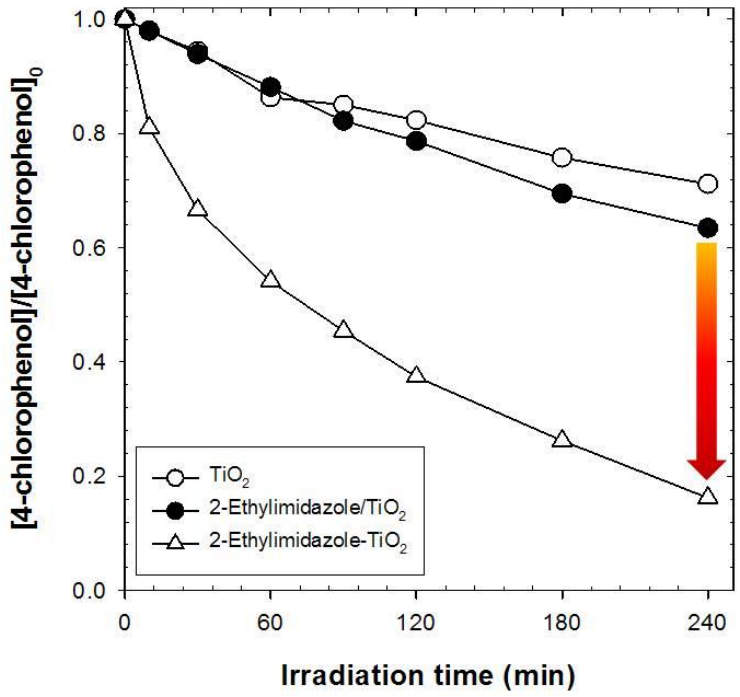

Figure 13. Degradation of 4-chlorophenol as target compound by TiO_2 (P25) and 2-ethylimidazole-TiO_2 in accordance with different pH conditions (>400 nm)

$[TiO_2]_0$ = 0.5 g/L; $[4\text{-chlorophenol}]_0$ = 10 μM; [Fluorescent lamp : 6 ea]; [Reaction time : 4 h]

In the case of various target compounds in Figure 14, 2-ethylimidazolethe-TiO_2 could degrade 4-chlorophenol, phenol, also, acetaminophen very well excepting for benzoic acid and carbamazepine. It implies that the formation of strong OH radicals was a weak because the slight degradation of

carbamazepine and benzoic acid could be accomplished only by usage and formation of potent oxidant. However, it could be interpreted as selective-degradable photocatalyst.

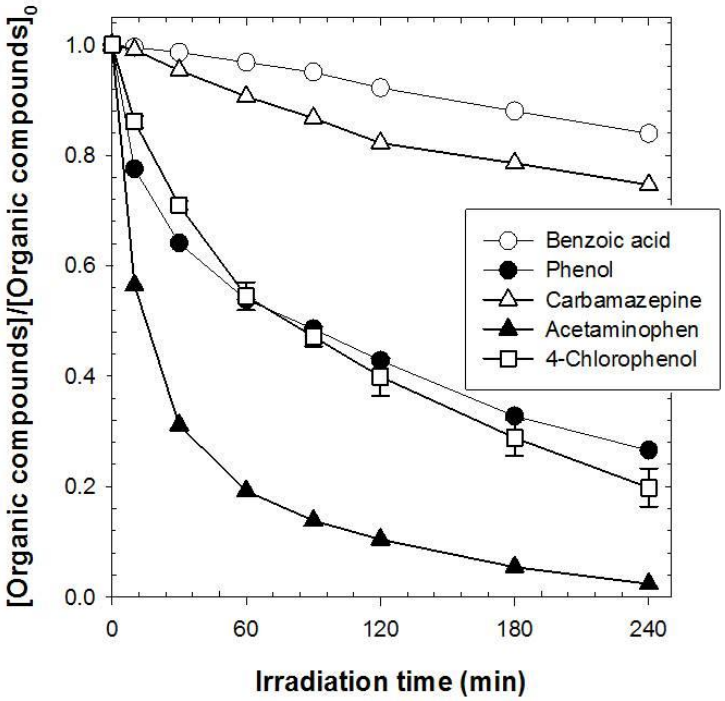

Figure 14. Degradation of various target compounds by 2-ethylimidazole-TiO_2 under the visible light condition (>400 nm)

$[TiO_2]_0$ = 0.5 g/L ; $[Benzoic\ acid]_0$ = $[Phenol]_0$ = $[4\text{-}Chlorophenol]_0$ = $[Acetaminophen]_0$ = $[Carbamazepine]_0$ = 10 μM ; [Fluorescent light : 6 ea] ; [Reaction time : 4 h]

Furthermore, the reusability test of 2-ethylimidazole-TiO_2 for the better performance as a catalyst was experimented for 4 times test repeatedly. In Figure 15, there is the data of the degradation of 4-chlorophenol for reusability of 2-ethylimidazole-TiO_2 under visible light condition. In that experiment, 1 uM of 4-chlorophneol was initially set for the quick analysis of trends. As shown below, even though the efficiency regarding the degradation of target compound was the better in 2-ethylimidazole-TiO_2 case, the reusability would be dramatically got lower after 1 usage. However, in the case of bare TiO_2 (P25), it shows very stable and repeat efficiency during degradation of target compound but this material was very weak as ever. That is, pure TiO_2 could decompose only about 30% within 1 hour. It was expected that the role of 2-ethylimidazole as nitrogen dopant was not pretty strong just after 1 usage. So, the recombination of the holes and electrons would occur easily on the surface of 2-ehtylimidazole-TiO_2 nanoparticles.

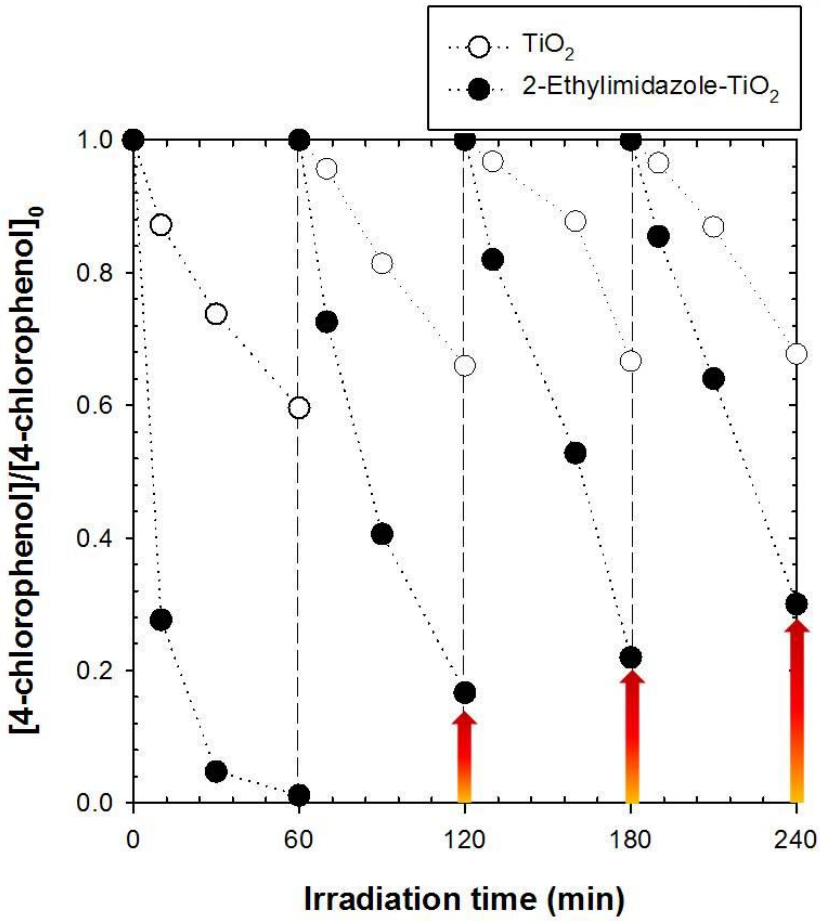

Figure 15. Degradation of target compounds for reusability test by 2-ethylimidazole-TiO_2 under the visible light condition (>400 nm)

$[TiO_2]_0$ = 0.5 g/L ; $[4\text{-Chlorophenol}]_0$ = 1 μM ; [Fluorescent light : 6 ea] ; [Reaction time : 4 h]

Moreover, its application for microcystin-LR was tried to solve the problem that harmful cyanobacterial toxins (e.g., microcystins) have raised concerns about the safety of drinking water resources. In Figure 16, these data could demonstrate the degradation of microcystin-LR in accordance with different pH roles under visible light irradiation. In advance, as mentioned reason of initial concentration of microcystin-LR set 100 ppb, it would be referred by the international standard of World Health Organization (WHO). Anyway, as shown in Figure 16, if the pH condition was lower, the photocatalyst could have the better efficiency in case of both bare TiO_2 and 2-ethylimidazole-TiO_2. In reality, pH condition is very important to titanium dioxide because the states of charge on the surface of TiO_2 would be changed in accordance with high or low pH condition in general. Thus, they react mainly with the adsorbed species. In this case, two materials ware activated very well under low pH condition. The efficient degradation of microcystin-LR could prove the certain part of nitrogen doping by 2-ethylimidazole, narrowed band gap, and visible light activity. Furthermore, 2-

ethylimidazole-TiO_2 was compared for proving the better performance of material with previously existing N-doped TiO_2.

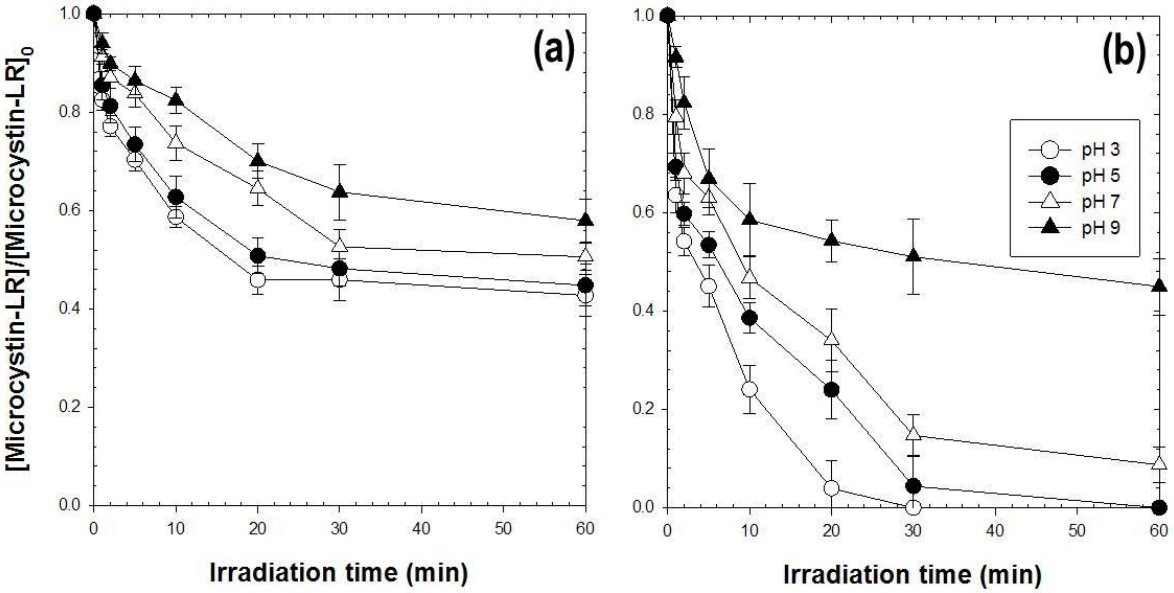

Figure 16. Degradation of microcystin-LR as a function of pH under visible light by TiO_2 (P25) (a) and 2-ethylimidazole-TiO_2 (b) (>400 nm)

$[TiO_2]_0$ = 0.5 g/L; $[Microcystin\text{-}LR]_0$ = 100 ppb; [Xenon lamp : 150 W]; [Reaction time : 1 h]

First, N-doped TiO_2 was made by modifying Degussa P25 contained dodecylamine as a nitrogen source at 350 ℃ (Choi *et al*., 2007). Secondly, N-doped TiO_2 was fabricated by a sol-gel method included ammonium hydroxide source (Kim *et al*., 2014). Thirdly, N-doped TiO_2 was modified by a sol-gel method. It used TTIP : Ethanol : HNO_3 : H_2O : dopant (urea) to synthesize (Ananpattarachai *et al*., 2009). These three N-doped TiO_2 photocatalysts were evaluated by the comparison of the efficiency on the papers separately. After that, all of experiments were fulfilled for finding out the best photocatalyst. As shown in Figure 17 below, the loading quantity of photocatalyst was 0.5 g/L and initial concentration of microcystin-LR was set 100 ppb under visible light irradiation condition by Xenon lamp. As a result, 2-ethylimidazole-TiO_2 was appraised as the best visible light response. The efficiency of it was the better than that of others. In other words, bare TiO_2 (P25) showed the worst performance under the visible light condition. However, like Figure 17 (b), bare TiO_2 (P25) was estimated the second performance under no cut-off condition contained UV region. It means that the band gap energy of bare TiO_2 certainly is broader than that of other N-doped TiO_2. Plus, 2-ethylimidazole-TiO_2 would be regarded the best photocatalyst in two conditions. 2-ethylimidazole-TiO_2 perfectly decomposed just for 1 hour under the only visible light irradiation and briefly during

20 min under the condition contained UV light. It shows the greater efficiency rather than bare TiO_2 (P25). This factor was thought as obtained excellent performance photocatalyst.

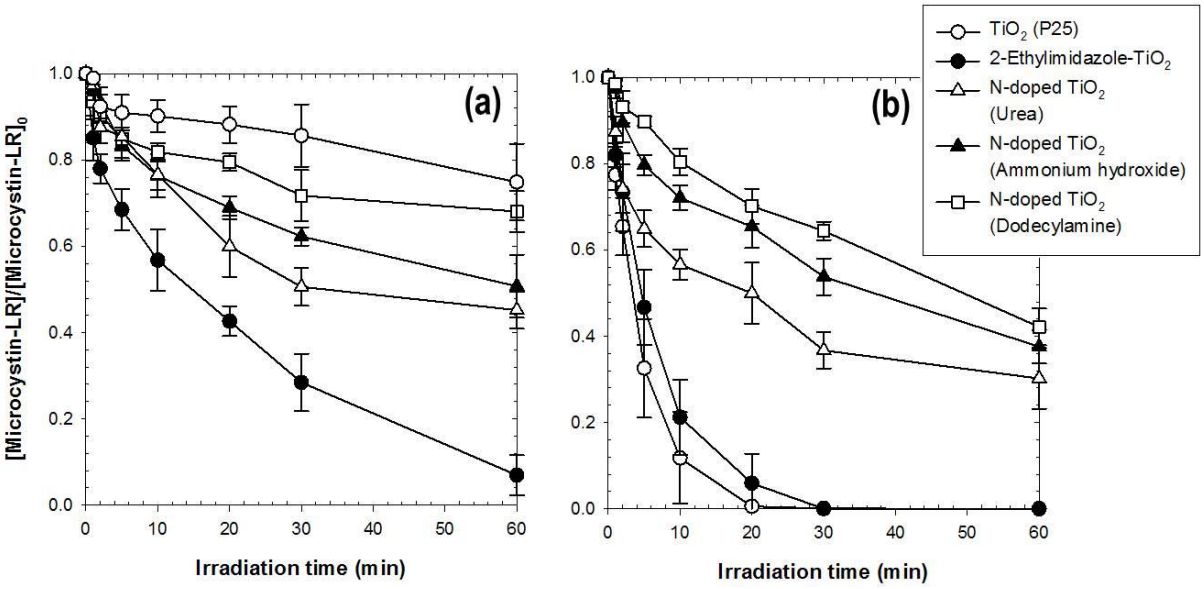

Figure 17. Degradation of microcystin-LR with cut-off filter (a) and without cut-off filter (b) by TiO_2 (P25) and various N-doped TiO_2 (>400 nm)

$[TiO_2]_0$ = 0.5 g/L; $[Microcystin\text{-}LR]_0$ = 100 ppb; [Xenon lamp : 150 W]; [Reaction time : 1 h]

All of TiO_2 was analyzed by comparing with X-ray photoelectron spectroscopy data on original value in each paper. XPS spectra of bare TiO_2 and four N-doped TiO_2 samples involved in 2-ethylimidazole-TiO_2 are shown in Figure 18 and 19 partially. The surfaces of all N-doped TiO_2 samples are consisted of titanium, oxygen, carbon and nitrogen compositions. No signal was only detected in regard with nitrogen source in the bare TiO_2 (P25). The peaks in Figure 19 show the bigger N 1s signals of the XPS spectra data. The intensity of the N 1s signals of N-doped TiO_2 of Choi et al. and 2-ethylimidazole-TiO_2 was more prominent rather than the weak intensity of N-doped TiO_2 by papers of Ananpattarachai and Kim. The 400.1 eV of binding energy of N 1s was detected in the photocatalyst of Choi and 2-ethylimidazole-TiO_2. It tacitly means formation of Ti-N-O bond on the surface of TiO_2. In other words, this analysis implies that the materials of Ananpattarachai and Kim would have different union combinations. From previous studies, typical binding energies below 397.5 eV are assigned to Ti-N. Therefore, all N-doped TiO_2 fabricated by this job process could be classified as N-doped TiO_2 involved in internal nitrogen. The quoted structure of this type titanium would be considered as the binding of nitrogen source to oxygen atom lattice in the circumstance of Ti-N-O and O-Ti-N.

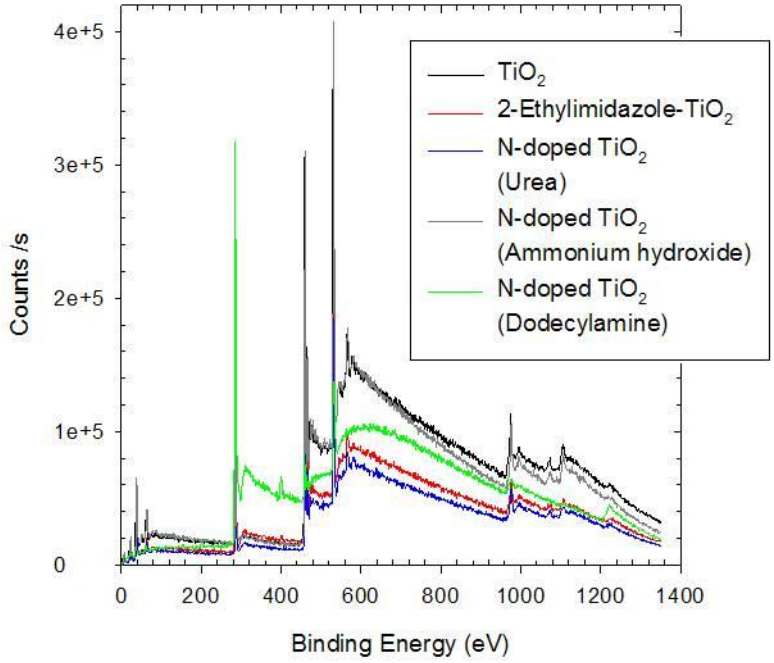

Figure 18. XPS spectra of various N-doped TiO_2 and TiO_2 (P25)

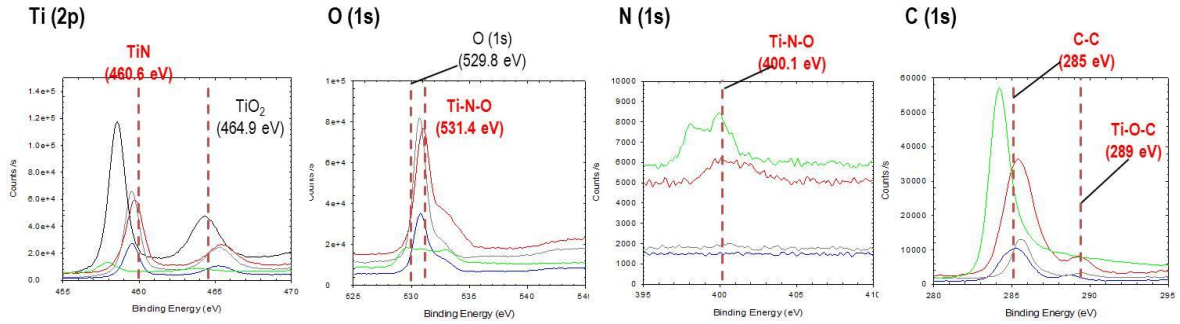

Figure 19. XPS spectra of Ti (2p), O (1s), N (1s) and C (1s) for various N-doped TiO_2 and TiO_2 (P25)

The content percentage of nitrogen atom in all TiO_2 as well as the atomic ratio of Ti, O, C and N atomic rate is demonstrated in Table 6. 2-ethlimidazole-TiO_2 would be expected to show the greatest content of four N-doped photocatalysts. This analysis information could propose that the chemical organization such as nitrogen content of N-doped TiO_2 mainly was consist of the molecular structure and the accessibility in regard with the nitrogen atoms to interact on the titania precursor.

Table 6. All XPS analysis of various N-doped TiO_2 and TiO_2 (P25)

Material	C (%)	N (%)	O (%)	Ti (%)
TiO_2 (P25)	30.63	-	48.81	20.08
2-Ethylimidazole-TiO_2	56.76	2.67	330.91	9.62
N-doped TiO_2 (Ammonium hydroxide)	26.51	0.30	42.97	17.39
N-doped TiO_2 (Urea)	46.80	0.50	38.79	13.92
N-doped TiO_2 (Dodecylamine)	81.47	5.07	11.08	1.38

1.4. Mechanism analysis

From previous studies of Sun and Bolton, the photocatalytic formaldehyde formation in the dispersions of TiO_2 nanoparticles would lead to the quantum yield value of OH radical regarded as the important intermediate in regard with oxidant. 2-ethylimidazole-TiO_2 was tested by using the general oxidation reaction in order to check the radical activity. Figure 20 explains that the concentration of formaldehyde linearly increases in the presence of photocatalyst with irradiation time. Therefore, the specific reaction rate would be taken in accordance with the slope of the straight lines as mentioned in Figure 20. Nitrogen doping obviously has slightly accelerating effect on the formaldehyde formation under visible light in TiO_2 photocatalyst. Additionally, the capacity of OH radical formation was decided by using benzoic acid reagent, which engages OH radical by taking the key reactant called 4-HBA (Bubacz *et al*., 2013). As shown below Figure 20, it explained that there was a weak OH radical effect because the production concentration of 4-HBA would be only approximately 0.3 micro moles for 1 hour under visible condition under Xenon lamp. In other words, when referred to previous studies, the effect and formation of OH radical would be inadequate in the case of 2-ethylimidazole-TiO_2.

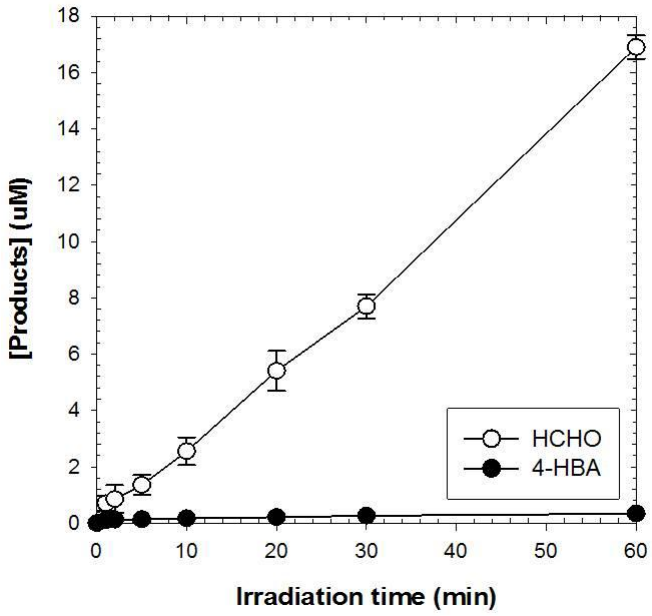

Figure 20. Production of formaldehyde and 4-hydroxy-benzoic acid by 2-ethylimidazole-TiO_2 under visible light (>400 nm)

$[TiO_2]_0$ = 0.5 g/L; $[Benzoic\ acid]_0$ = 10 mM; $[Methanol]_0$ = 200 mM; [Xenon lamp : 150 W]; [Reaction time : 1 h];

Plus, methanol or tert-butyl alcohol is widely employed as the general hole scavengers in photocatalytic studies (Choi *et al*., 1994). The photocatalysis of methanol in regard with TiO_2 is also prominent in environmental remediation and reforming reaction product. From Figure 21, similar trend was certainly found out in case of microcystin-LR. If the effect of OH radical was strong, the differences of the efficiency would be great between with radical scavenger and without radical scavenger. However, in this case, below data implies that the influence of the radical is pretty weak.

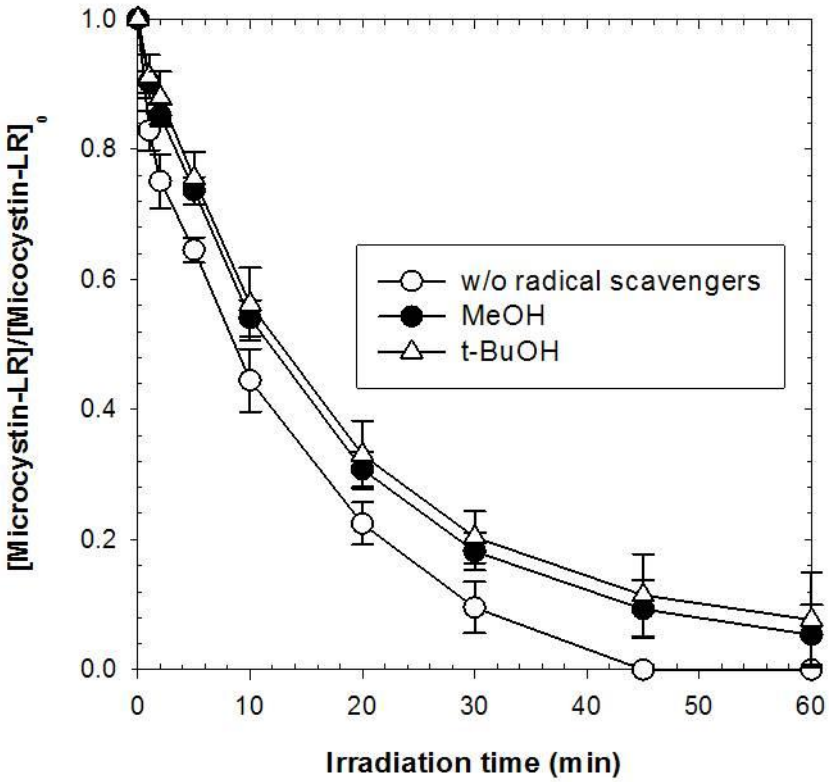

Figure 21. Radical scavenging effect by using microcystin-LR as target compound under visible light (>400 nm)

$[TiO_2]_0$ = 0.5 g/L; [Microcystin-LR] = 100 ppb; [tert-Buthanol]$_0$ = 200 mM; [Methanol]$_0$ = 200 mM; [Xenon lamp : 150 W]; [Reaction time : 1 h]

Finally, the following possible mechanism was proposed regarding 2-ethylimidazole-TiO_2. In this study, some experiments could have additionally attempted to prove the mechanism in regard with visible light response of 2-ethylimidazole-TiO_2 nanomaterials. Actually, there are a lot of papers that concentrated on the photocatalytic response mechanism of nitrogen doped TiO_2. Accordingly, the crystalline structure of TiO_2 was modified by the simple method, which leads to new mid-level N 2p band. As a result, the band gap of TiO_2 was narrowed and derived the enhanced visible light. Also, the generation of Ti^{3+} donor band derived photo-absorption on N-doped TiO_2 because many electron-hole

pairs were created by visible light activation (Yang *et al*., 2006). The charge carrier rapidly diffuses on the surface of TiO_2 if not trapped or recombined. The presence of many electrons could bring about Ti^{4+} reduction and Ti^{3+} generation in regard with TiO_2 anatase phase with continuous generation of Ti^{3+}, 3d orbital, which was assigned to be less than the conduction band bottom. The electrons could be moved through this conduction band to Ti^{3+} state. Eventually, we can ensure that the nitrogen and Ti^{3+} could cooperatively affect to narrow the band gap of N-doped TiO_2. As mentioned before, nitrogen doping could derive the oxygen vacancies generation. This paramagnetic property may assist to the enhanced visible light response. As shown in Figure 22, the electron directly moves to the conduction band and O_2 to generate the superoxide ions (O_2^-). Then, holes (h^+) react OH^- species to make OH radical slightly. As a result, the direct hold oxidation cooperatively could assist to have the higher visible light response with slight OH radical effects.

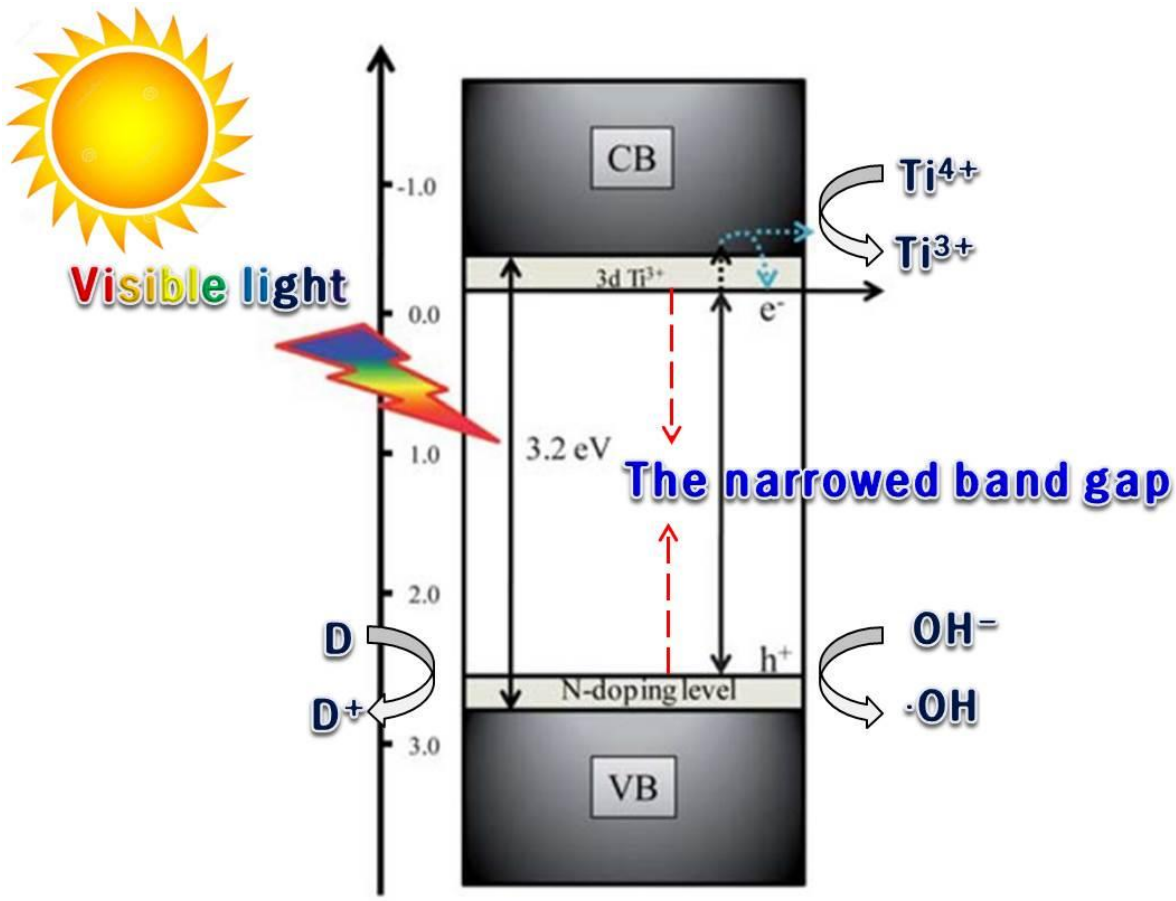

Figure 22. Diagram for demonstrating a mechanism of 2-ethylimidazole-TiO_2 in regard with nitrogen doping

2. Synthesis of Co-H_2O_2-TiO_2 and its application in visible light response photocatalysis of organic compounds

2.1. Optimization of material

In the previous study for this material, the optimization of H_2O_2-TiO_2 was already progressed. So, the concentration of hydrogen peroxide for fabricating H_2O_2-TiO_2 was certainly optimized as the one molarity. Plus, it is very novel to focus on the rate constant of 4-chlorophenol degradation in regard with various commercial photocatalysts. In addition, the different cobalt concentration was controlled by using cobalt nitrate. From Figure 23, cobalt doped H_2O_2-TiO_2 was optimized through experiments in regard with the comparison of the degradation's efficiency. Actually, the photo-degradation of 4-chlorophenol as specific target compound was fulfilled under the visible light irradiation with cut-off filter (>400 nm). H_2O_2-TiO_2 treated by the different cobalt concentration was utilized for optimization of cobalt concentration. As shown in Figure 25, when the concentration of cobalt was 0.2 mM, the efficiency of material was the best. On the basis of the standard concentration (0.2 mM), the degradation efficiency of the remainders decreased gradually (Hamal *et al*., 2011).

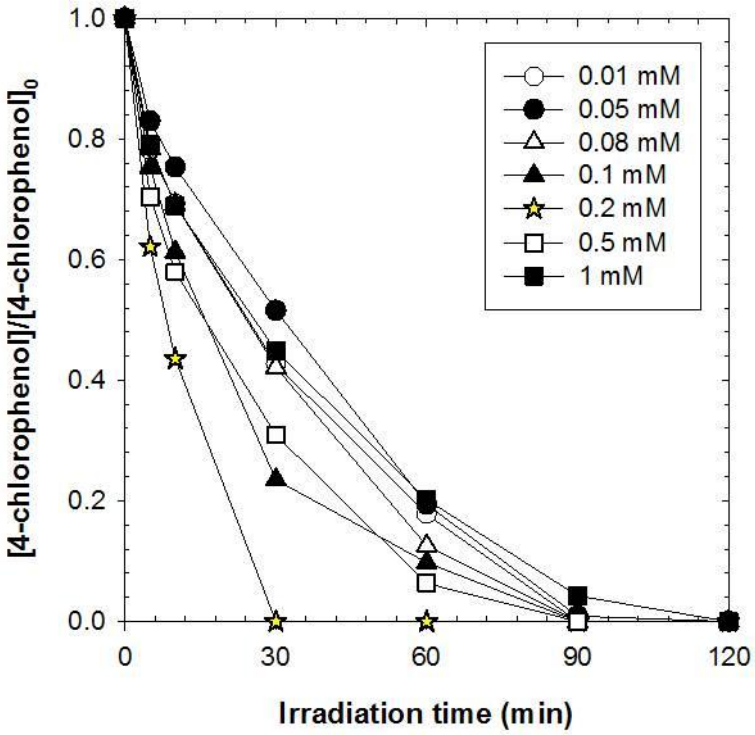

Figure 23. Comparison of the degradation efficiency in accordance with different ratio of concentration of cobalt under the visible light (>400 nm)

$[TiO_2]_0$ = 0.5 g/L; $[4\text{-chlorophenol}]_0$ = 10 μM; [Fluorescent lamp : 6 ea]; [Reaction time : 2 h]

Additionally, it was clearly compared as pseudo-first order rate constant (k value (min^{-1})) like bar graph of Figure 25. As the procedures, after finished cobalt doping of H_2O_2-TiO_2 by sol-gel method, the color was changed washy-yellowish as shown Figure 24. In reality, this color was showed whenever some metal ion doping was tried such as platinum, copper and ferric ion and so on by a sol-gel method (Choi *et al*., 2010). It was expected more photo-adsorption of material and more response under visible light irradiation condition. However, the degrees of the color change were not related with the quantity of cobalt nitrate or other metal ion's concentration. In other words, it retained similar colors in spite of different concentration condition.

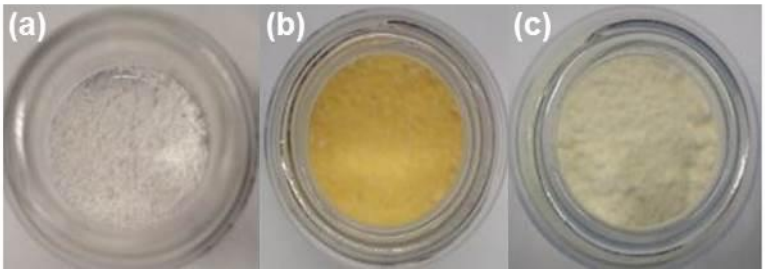

Figure 24. Different colors of TiO_2 (P25) (a), H_2O_2-TiO_2 (b) and Co-H_2O_2-TiO_2 (c)

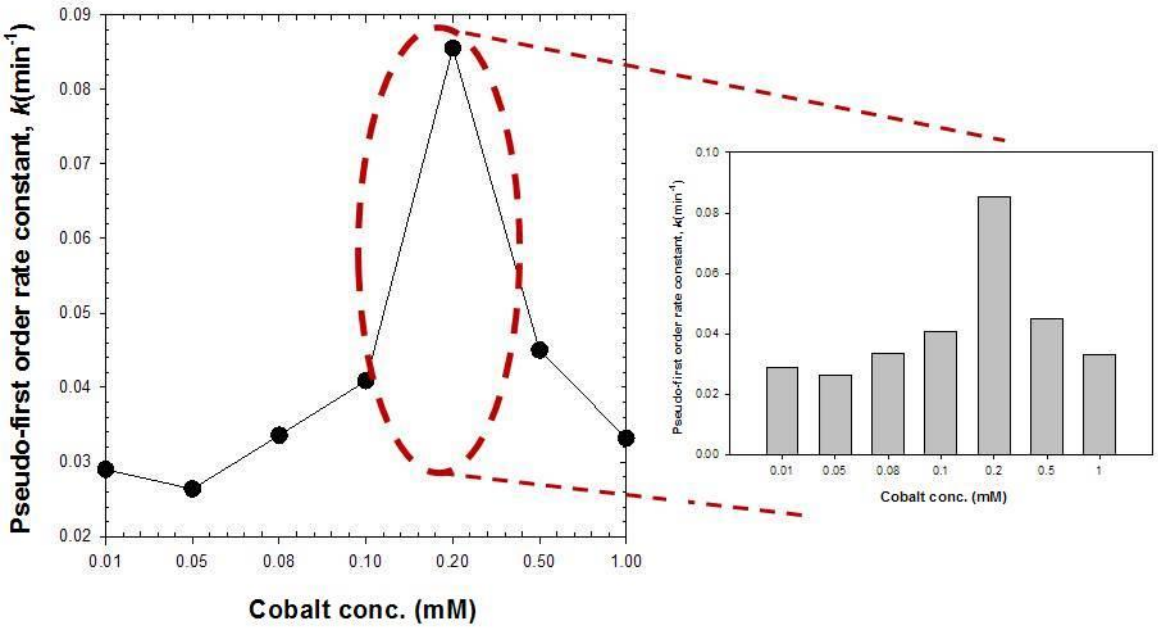

Figure 25. The efficiency of Co-H_2O_2-TiO_2 fabricated under different concentration of cobalt the visible light (>400 nm)

2.2 Characterization of material

In Figure 26, overall, X-ray diffraction spectral data of the fabricated materials was fulfilled by checking just for the anatase formation. This result could be indicated on the base of the material crystallite size. The tinier the crystallite size was, the better the dispersion of some doping was in natural. The most intensive peak is shown in below XRD data exactly in Figure 26. As shown in the pattern of XRD, it contained anatase with the poor crystallinity due to the low temperature condition to fabricate Co-H_2O_2-TiO_2. This result also demonstrates that the formation of rutile and anatase was deeply influenced by calcination procedure and some temperature condition to calcinate.

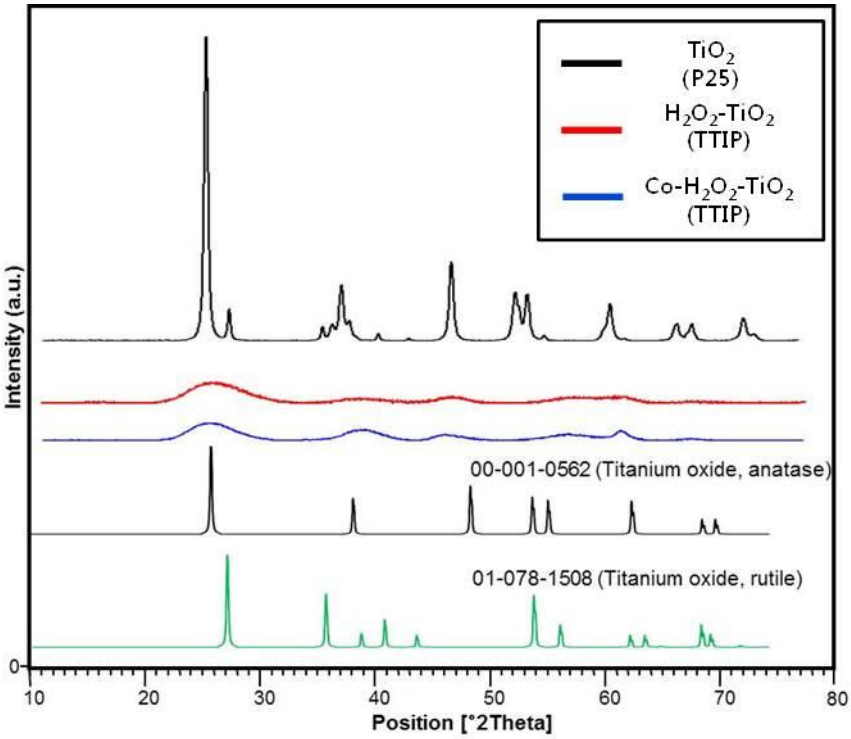

Figure 26. X-ray diffraction pattern of TiO_2 (P25), H_2O_2-TiO_2 and Co-H_2O_2-TiO_2

To sure the specific chemical valence situation of Ti, O, C and Co, X-ray photoelectron spectroscopy (XPS) analysis of three materials was respectively analyzed in regard with element. XPS peak data of cobalt doped H_2O_2-TiO_2 is shown in Figure 27 and 28. The Ti 2p XPS spectrum in Figure 28 signified that titanium is present as Ti^{4+}. The O 1s peak with the specific shoulder explained that oxygen exists as O_2^-. In other words, O-Ti and OH-Metal lattice could consist of the surface structure. The C 1s implied that most carbon would exist as the graphitic carbon. The bulk elemental analysis of cobalt doped H_2O_2-TiO_2 involved cobalt (0.79 at. %) as shown in Table 7. The results indicated that the doped cobalt ion would be evenly distributed on the material. Regarding cobalt elements, it is too difficult to distinguish Co^{2+} or Co^{3+} species through Co 2p 3/2 core level binding energy value at 782.1 eV. Actually, some specific feature in regard with Co 2p will support to

recognize Co^{2+} and Co^{3+} oxidation situation. If Co^{2+} specie exists, the specific XPS peaks (Co 2p) could demonstrate the clear peaks data like a shake-up satellite at higher binding energies. Overall, cobalt doped H_2O_2-TiO_2 was proved through these facts in regard with cobalt doping effects from XPS spectra and the analysis of atomic ratio.

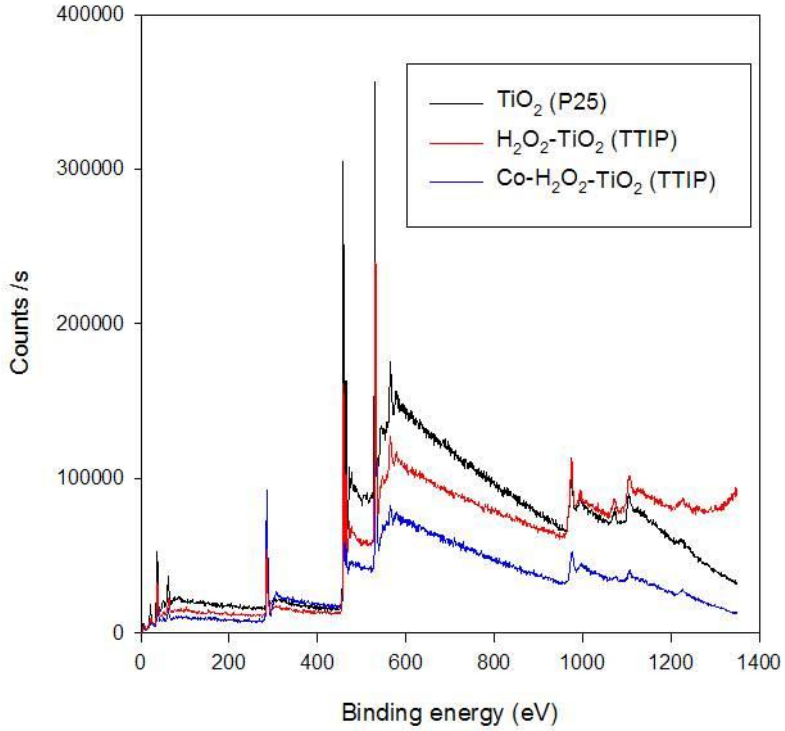

Figure 27. XPS spectra of TiO_2 (P25), H_2O_2-TiO_2 and Co-H_2O_2-TiO_2

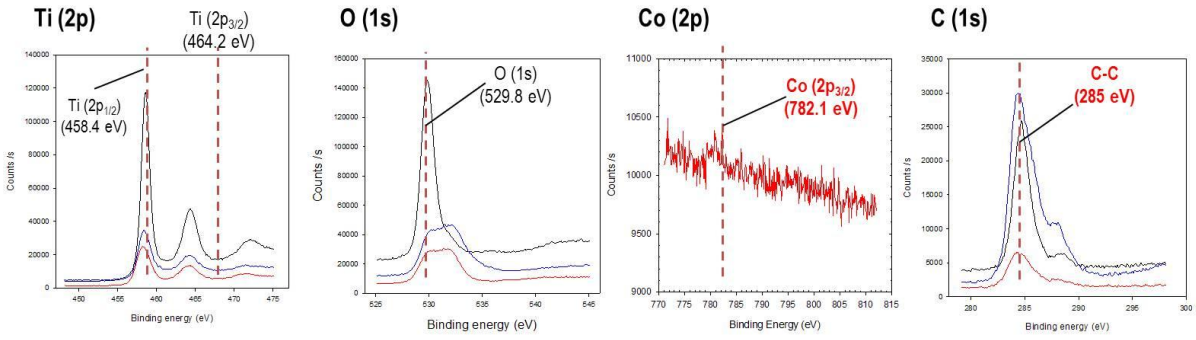

Figure 28. XPS spectra of Ti (2p), O (1s), N (1s) and C (1s) for TiO_2 (P25), H_2O_2-TiO_2 and Co-H_2O_2-TiO_2

Table 7. XPS analysis of TiO_2 (P25), H_2O_2-TiO_2 and Co-H_2O_2-TiO_2

Material	C (%)	Co (%)	O (%)	Ti (%)
TiO_2 (P25)	53.79	-	35.51	11.01
H_2O_2-TiO_2	36.41	-	48.54	15.06
Co-H_2O_2-TiO_2	29.25	0.79	54.59	15.37

To confirm the existence of the nano-sized composition, TEM images of three samples were obtained. First of all, it is clear that this sample was constituted as a very small nanoparticle in Figure 29 and the measured size is 20 nm and 50 nm. The formation of very tiny TiO_2 materials could support to transfer the photoelectron charge on the surface. Hence, it is expected that the doped cobalt could lead to high response activities for the contaminant remediation under visible light irradiation. Additionally, cobalt doped H_2O_2-TiO_2 showed image (f) of Figure 26 like a pike. It is very interesting because this shape was never reported as TEM images of photocatalyst. As expected, it implies that cobalt nitrate of fabrication procedure directly influences the surface of material. Also, this results was interpreted well-doped TiO_2 when comparing with others. Plus, EDS images supported and showed well the distribution map of cobalt in Figure 30.

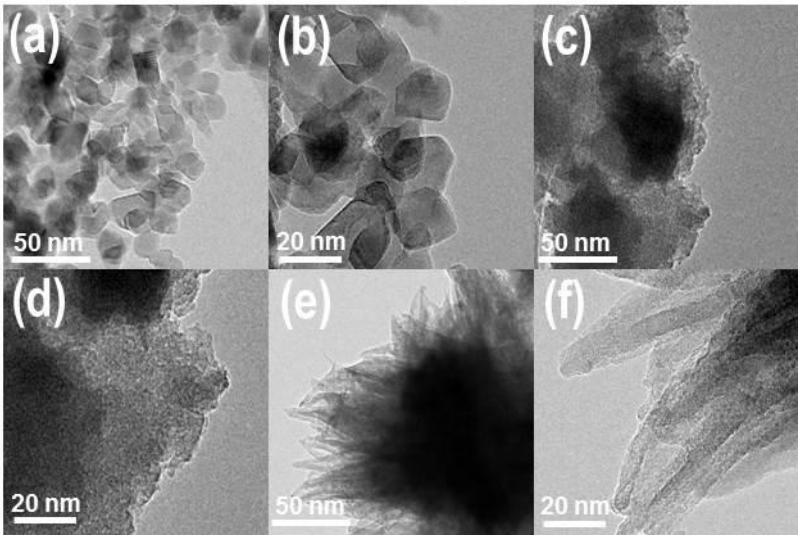

Figure 29. TEM images of 50 nm (a), 20 nm (b) of TiO_2 (P25), and 50 nm (c), 20 nm (d) of H_2O_2-TiO_2 and 50 nm (e), 20 nm (f) Co-H_2O_2-TiO_2

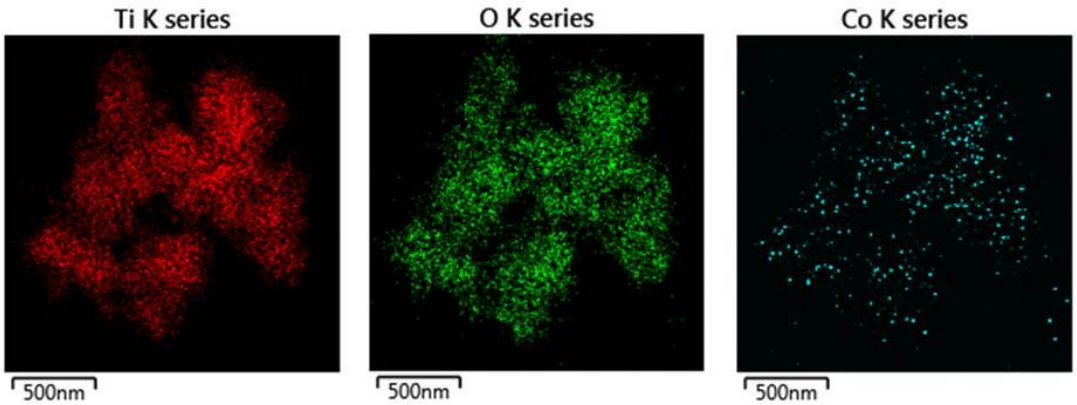

Figure 30. EDS images contained content of Ti, O and Cobalt of Co-H_2O_2-TiO_2

In addition, UV-Vis diffuse reflectance analysis showed the optical absorption of nano-materials under visible light area in Figure 31. The result could demonstrate that all nano-size photocatalysts can lead its visible light response for the degradation on target compounds. As shown in Figure 31, it especially exhibited the extended photo-absorption capacity in visible light region (420 - 580 nm). From this result, Co-H_2O_2-TiO_2 was clearly proved its visible response when comparing to other materials.

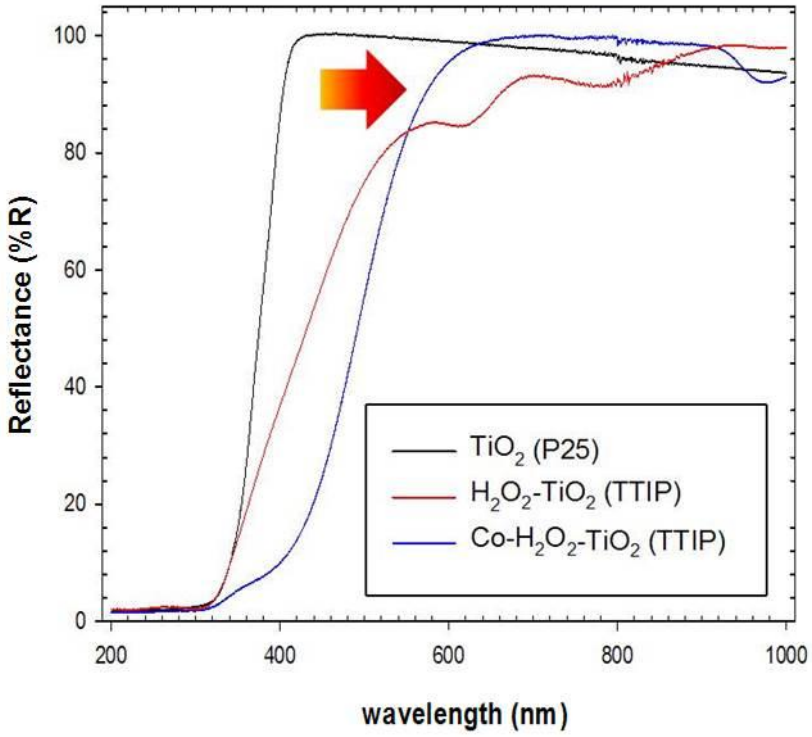

Figure 31. Diffuse reflectance spectra of TiO_2 (P25), H_2O_2-TiO_2 and Co-H_2O_2-TiO_2

The photocatalytic activity of H_2O_2-TiO_2 under visible light irradiation is associated with this photo-absorption under visible area (Tachikawa *et al*., 2004). However, the poor photocatalytic response of the anatase powder should not be overlooked under visible light despite of its absorption capacity in visible region with hydrogen peroxide treatment. Therefore, further information about the generated species is necessary to analyze mechanism on the hydrogen peroxide treated TiO_2 surface.

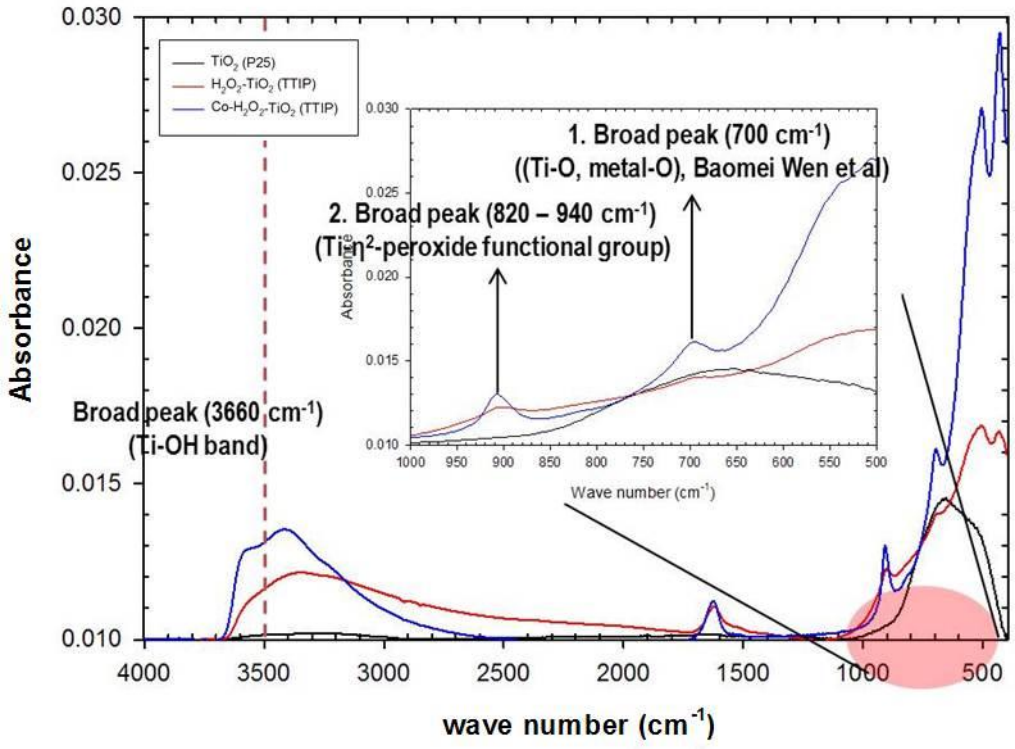

Figure 32. FTIR analysis of TiO_2 (P25), H_2O_2-TiO_2 and Co-H_2O_2-TiO_2

In order to get the exact report in regard with the formation of Ti-peroxide on the surface, its FT-IR spectra data was totally measured respectively (Ohno *et al*., 2001). Figure 32 demonstrates the clear broad peak (700 cm^{-1}) for Ti-O, metal-O bonds and Ti-η^2-peroxide functional group bonds between the difference spectra of bare TiO_2 (P25) and H_2O_2-TiO_2 samples. It implies that hydrogen peroxide treatment and cobalt doping were fulfilled very-organized. The band in the range (960 - 690 cm^{-1}) was hailed to dissimilar Ti-peroxo species. Ti-η^2-peroxide was reported to take the absorption bands in the range (935 - 790 cm^{-1}). In the opposite sense, Ti-μ-peroxide was also informed of getting the absorption band in the range (780 - 710 cm^{-1}), which was usually explained in regard with solid state of peroxide. Plus, the absorption band in the ranges (950 - 830 cm^{-1}) was described as the increasing the vibration signal of -O-O- bond of Ti-μ-peroxide and Ti-η^2-peroxide as shown in Figure 32. The tiny absorption in the region (950 - 800 cm^{-1}) may be owing to the included rutile component in the photocatalyst. Obviously, a broad peak (700 cm^{-1}) could be considered with δ (Ti-O, metal-O).

Plus, the clear peaks (3400 cm^{-1} and 1640 cm^{-1}) demonstrated the characteristic absorption of δ (-OH) and δ (-O-H) functional organizations. Actually, it was owing to the hydrated species such as Ti-OH. The enhanced signal of the peak (700 cm^{-1}) could be accepted as a result of the strong mutual interaction between cobalt and oxygen. Accordingly, it was guessed that the cobalt doping modifies the hydrophilic property on the surface.

2.3 Processing efficiency evaluation

To make certain the enhanced photocatalytic response of the photocatalysts, the decomposition of 4-chlorophenol was mainly experimented with visible light of fluorescent light mounted cut-off light filter (>400 nm). As shown in Figure 33, when comparing to pure TiO_2 (P25), Co-H_2O_2-TiO_2 can be seen that it could decompose of 4-chlorophenol perfectly only within 30 min. The concentration of target compound was correctly analyzed by using high performance liquid chromatography like previous cases. Actually, the photocatalytic response of cobalt doped H_2O_2-TiO_2 was greatly improved under visible light irradiation as compared to the bare TiO_2 (P25), which suggests that the degrees of cobalt doping had an distinct impact on the photocatalytic response of TiO_2. In addition, this material could perfectly degrade 4-chlorophenol (10 μM) for half hour. Also, it shows the perfect decomposition efficiency of same target compound just for ten minutes under Xenon lamp condition called one sun condition. As shown in Figure 34, there are the data in regard with the degradation of 4-chlorophenol with cut-off filter (a) and without cut-off filter (b) by commercial TiO_2 (P25), H_2O_2-TiO_2, and cobalt doped H_2O_2-TiO_2 under one sun condition.

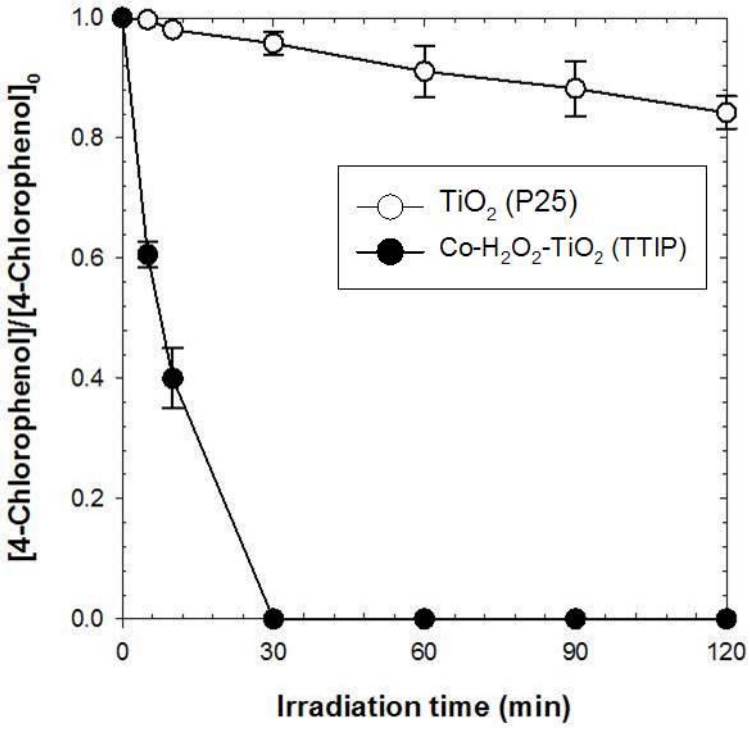

Figure 33. Degradation of 4-chlorophenol by TiO_2 (P25) and Co-H_2O_2-TiO_2 under the visible light condition (>400 nm)

$[TiO_2]_0$ = 0.5 g/L; $[4\text{-chlorophenol}]_0$ = 10 μM; [Fluorescent lamp : 6 ea]; [Reaction time : 2 h]

In detail about Figure 34 (a), when experimented with 400 nm cut-off filter only for usage of visible light, H_2O_2-TiO_2 and cobalt doped H_2O_2-TiO_2 could degrade all 4-chlorophenol very fast. H_2O_2-TiO_2 perfectly decomposed 4-chlorophenol (10 μM) for 2 hours. Next, it was totally degraded within 30 minute under no cut-off filter condition. However, when comparing with the commercial TiO_2 (P25), the rate constant of cobalt doped H_2O_2-TiO_2 was not better than the bare TiO_2 (P25). It was shown similarly in Figure 34 (b). Plus, H_2O_2-TiO_2 showed the third efficiency. If considering these data, cobalt doping positively influenced the efficiency enhancement of H_2O_2-TiO_2.

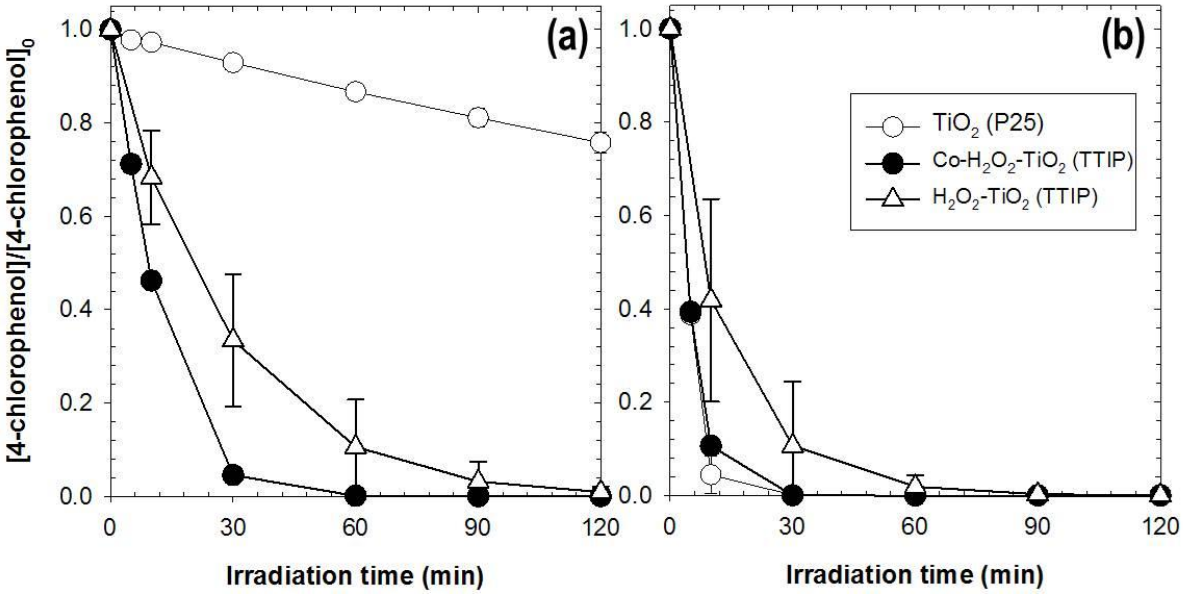

Figure 34. Degradation of 4-chlorophenol with cut-off filter (a) and without cut-off filter (b) by TiO_2 (P25), H_2O_2-TiO_2 and Co-H_2O_2-TiO_2 under Xenon lamp (>400 nm)

$[TiO_2]_0$ = 0.5 g/L; $[4\text{-chlorophenol}]_0$ = 10 μM; [Xenon lamp : 150 W]; [Reaction time : 1 h]

In the case of various target compounds in Figure 35, cobalt doped H_2O_2-TiO_2 could degrade 4-chlorophenol, phenol, microcystin-LR and acetaminophen very well except for benzoic acid and carbamazepine. It was expected that the formation of strong radicals (OH radical) was too feeble because the degradation of carbamazepine and benzoic acid as non-degradable organic material could be accomplished by formation of strong oxidant. As shown in Figure 35, well-degraded organic compounds (phenol, 4-chlorophenol, acetaminophen and microcystin-LR) were nearly perfectly decomposed before 1 hour under visible light condition. Especially, in this case of microcystin-LR, the efficiency of cobalt doped H_2O_2-TiO_2 was better than that of previous study (2-ethylimidazole-TiO_2). Even though it might be different in accordance with dopants, we expected that the effect of some metal doping was more effective than the effect of some non-metal doping.

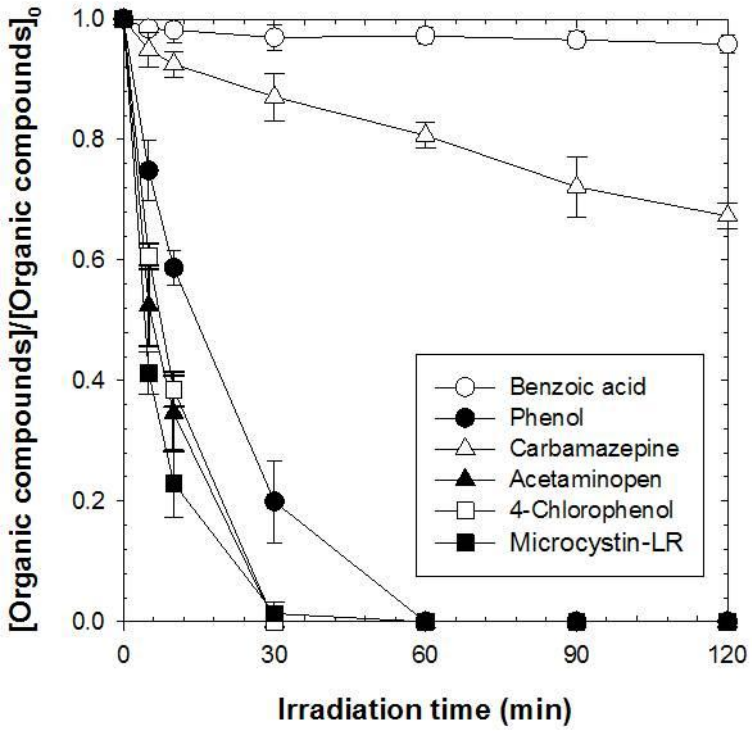

Figure 35. Degradation of various target compounds by Co-H_2O_2-TiO_2 under the visible light condition (>400 nm)

$[TiO_2]_0$ = 0.5 g/L ; $[Benzoic\ acid]_0$ = $[Phenols]_0$ = $[Acetaminophen]_0$ = $[Carbamazepine]_0$ = 10 μM ; $[Microcystin\text{-}LR]_0$ = 100 ppb ; [Fluorescent light : 6 ea] ; [Reaction time : 2 h]

Furthermore, the reusability test of cobalt doped H_2O_2-TiO_2 and H_2O_2-TiO_2 were experimented 4 times repeatedly for the better development. In Figure 36, there is the data of the degradation of 4-chlorophenol for reusability test by H_2O_2-TiO_2 under visible light condition. In this experiment, 4-chlorophneol (10 μM) was initially set for the exact comparison of trends under different condition. As proposed in Figure 36, even though the efficiency regarding the decomposition was the better in the case of cobalt doped H_2O_2-TiO_2, the reusability of them would be similarly lower gradually after 1 usage as same trends. However, as mentioned before, in the case of bare TiO_2 (P25), it shows very stable reusability during the repetitive degradation of target compound but this material had a weak efficiency as ever. Pure TiO_2 (P25) could decompose 4-chlorophenol only approximately 35% within 1 hour. It was expected that the role responsibility of cobalt doping decreased just after 1 experiment increasingly. First, if so, some fact was expected that the recombination of the holes and electrons would happen fast on the surface of cobalt doped H_2O_2-TiO_2 material through this phenomenon (Bingham *et al*., 2011). Additionally, the results of the degradation were attached to check the expendability of photocatalyst just by irradiation after 12 hours of TiO_2 dispersion.

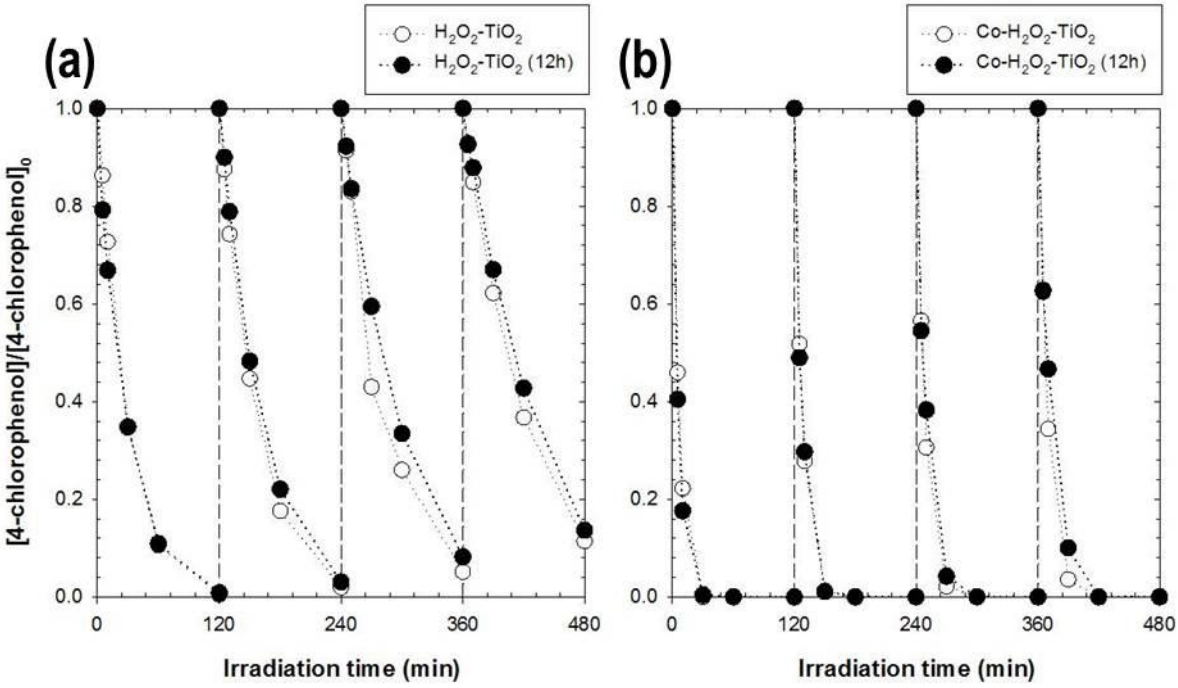

Figure 36. Degradation of target compounds for reusability test by H_2O_2-TiO_2 (a) and Co-H_2O_2-TiO_2 (b) under the visible light condition (>400 nm)

$[TiO_2]_0$ = 0.5 g/L ; [4-Chlorophenol]$_0$ = 10 μM ; [Fluorescent light : 6 ea] ; [Reaction time : 8 h]

As shown in Figure 37, it was experimented in accordance with different pH conditions. In detail, if pH condition was lower, the photocatalyst had the better efficiency in cases of cobalt doped H_2O_2-TiO_2 and H_2O_2-TiO_2. Actually, pH condition is very important to metal substances such as titanium dioxide because the states of charge on the surface of metal would be generally changed in accordance with high or low pH condition. The differences in the kinetic in accordance with pH conditions are so distinct as shown Figure 37 (a) and (b). In two cases, two materials were activated very well under low pH condition. Especially, in the case of cobalt doped H_2O_2-TiO_2, the efficiency at pH 3 was two times positive rather than the efficiency of pH 9. Also, these data were deeply related to zeta potential value under different pH conditions. In general, about the charge of titanium dioxide which has a surface of metal, if the condition of pH is the higher, the charge of the surface regarding titanium dioxide would be more negative. Additionally, it is influenced by target compounds because pKa value was numerous in accordance with the organic compounds respectively. In summary, these data obviously proved the role of cobalt doping and it also showed great enhancement of the photocatalytic efficiency by cobalt doping (Pettibone *et al*., 2008).

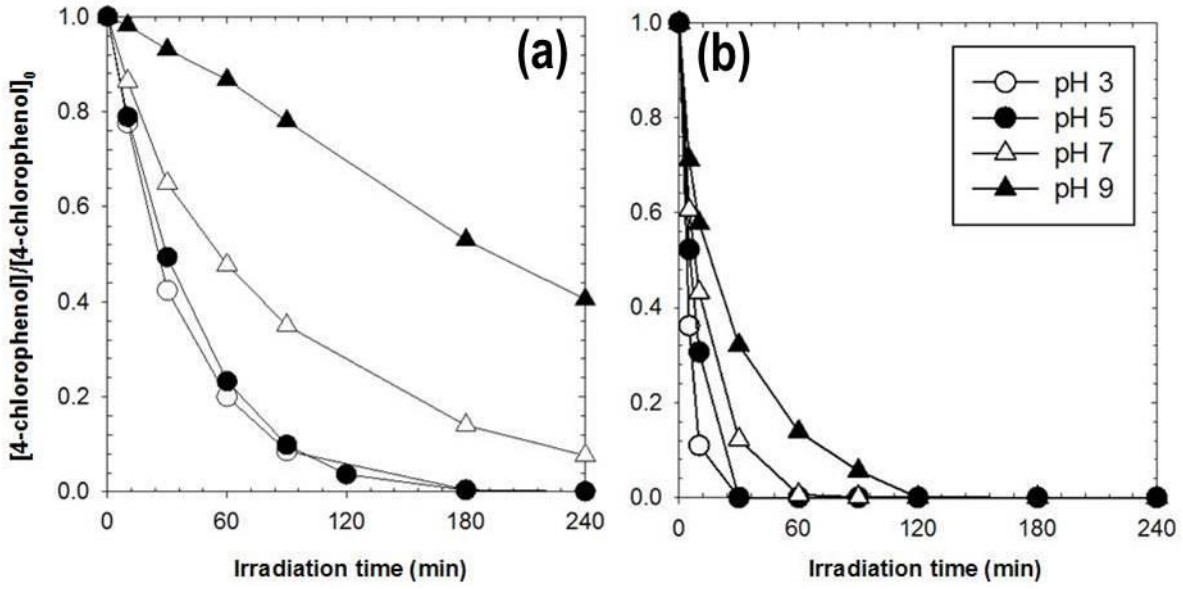

Figure 37. Degradation of 4-chlorophenol in accordance with different pH under visible light by H_2O_2-TiO_2 (a) and Co-H_2O_2-TiO_2 (b) (>400 nm)

$[TiO_2]_0$ = 0.5 g/L; [4-Chlorophenol]$_0$ = 10 μM; [Fluorescent light : 6 ea]; [Reaction time : 4 h]

2.4. Mechanism analysis

As shown in Figure 38, the aqueous TiO_2 suspensions containing light irradiation lead to the formaldehyde formation. The formaldehyde concentration would linearly go up with irradiation time. As mentioned in the paper of Sun and Bolton, this was quite early studied about the photocatalytic formaldehyde formation in the aqueous oxygenated TiO_2 nanoparticles. Cobalt doped H_2O_2-TiO_2 was minutely experimented by using the similar oxidation reaction for the purpose of inquiring the photocatalytic response. Figure 38 enters into details regarding the concentration growth of formaldehyde with illumination time. Therefore, the photochemical reaction rate is obtained with the line slope shown in Figure 38. Markedly, some metal doping could have the vivid impetus effect. Additionally, the generation capacity of OH radical would be expected by using benzoic acid and coumarin, which could capture OH radical to form the intermediates of reactions, 4-hydroxy benzoic acid (4-HBA) and 7-hydroxycoumarin. As shown in Figure 38 below, it demonstrated that there was a weak OH radical effect since the production concentration of 4-hydroxy-benzoic acid and 7-hydroxycoumarin would be only around below 0.1 μM for 2 hours under visible light irradiation condition by Xenon lamp. In other words, as referred to previous studies, when comparing with original TiO_2 (P25), the effect and formation quantity of OH radical would be relatively inadequate.

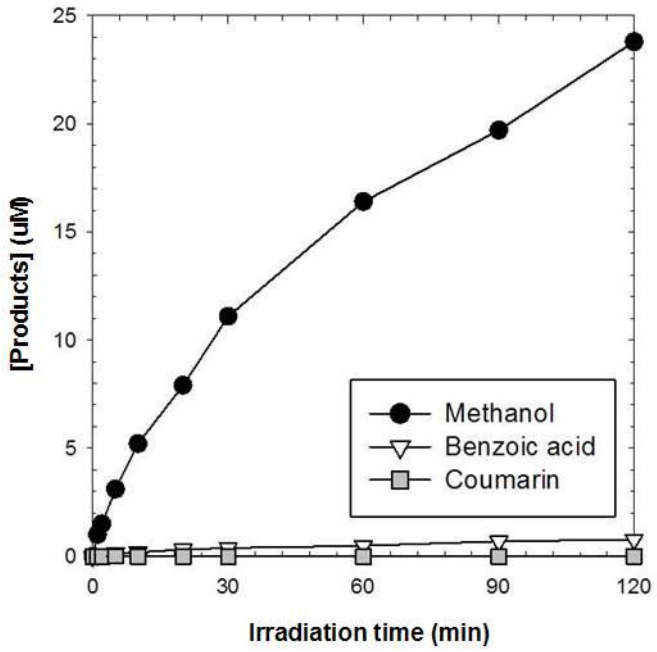

Figure 38. Formaldehyde production of Co-H_2O_2-TiO_2 by using 4-chlorophenol under visible light (>400 nm)

$[TiO_2]_0$ = 0.5 g/L; $[Benzoic\ acid]_0$ = 10 mM; $[Methanol]_0$ = $[Coumarin]_0$ = 200 mM; [Xenon lamp : 150 W]; [Reaction time : 2 h]

Plus, methanol or tert-butyl alcohol is widely utilized as the scavenger in photocatalytic studies on TiO_2. The photocatalysis of methanol related to TiO_2 is also outstanding in environmental remediation. As shown in Figure 39, almost similar trends were certainly found out despite of same target compound (4-chlorophenol). If the effect of some radicals was strong, there would be big differences between radical scavenger and no radical scavenger. However, in this case, these data imply that the influence of radicals is so weak certainly. Next, ascorbic acid is widely recognized to take a similar role. It could invigorate Fenton process and retard the flow of scavenge ocygen radicals (Santrucek *et al*., 1988).

Even if OH radical was more sensitive and powerful than superoxide radical, the role of superoxide has been importantly proposed in regard with the inflammation (Petrone *et al*., 1980). The main evidence was chiefly because of the scientific fact as OH radical scavenger were not associated with anti-inflammatory behavior (Oyanagui *et al*., 1982). It has been also shown that ascorbic acid and its derivative could react as superoxide radical scavengers, which consequently leads to the decrease of the efficiency regarding degradation of target compound. In reality, a liitle decrease of the efficiency was revealed by ascorbic acid as superoxide radical scavenger.

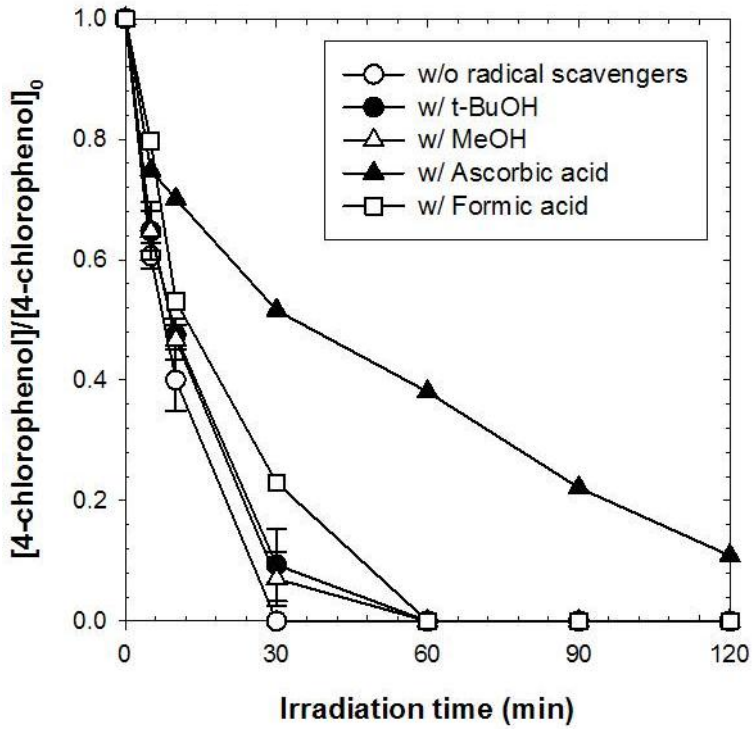

Figure 39. Effect of radical and hole scavengers by using 4-chlorophenol under visible light (>400 nm)

$[TiO_2]_0$ = 0.5 g/L; $[4\text{-Chlorophenol}]_0$ = 10 μM; $[\text{tert-Buthanol}]_0$ = $[\text{Methanol}]_0$ = $[\text{Ascorbic acid}]_0$ = $[\text{Formic acid}]_0$ =200 mM; [Fluorescent light : 6 ea]; [Reaction time : 2 h]; [pH_0 = 5.0]

Plus, in this experiment, formic acid was normally used as the scavenger to enhance the photocatalytic reaction. The experiments demonstrated that cobalt was effectively doped in H_2O_2-TiO_2. In the presence of formic acid, we could have some opinions that the photocatalytic reduction of cobalt can be appropriately performed from H_2O_2-TiO_2.

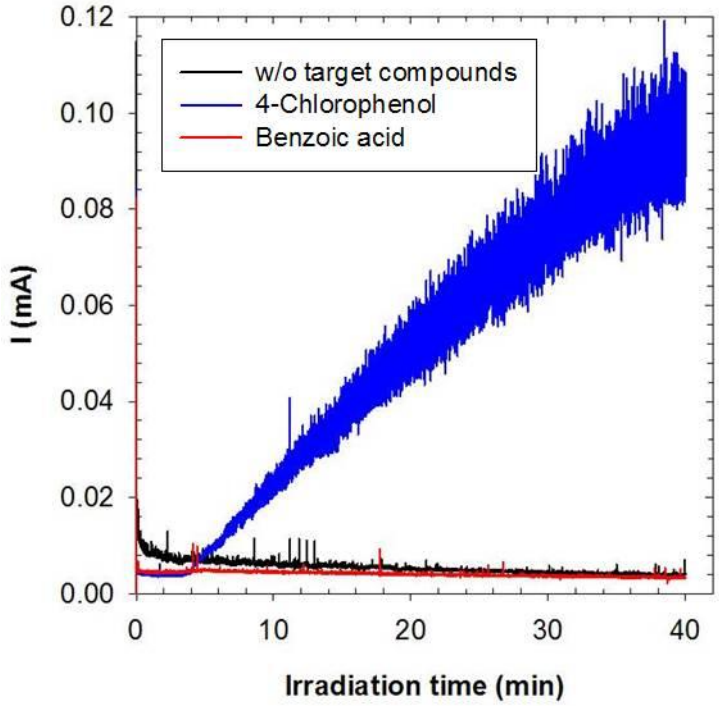

Figure 40. Photocurrent of Co-H_2O_2-TiO_2 by using 4-chlorophenol and benzoic acid under visible light (>400 nm)

$[NaClO_4]_0$ = 0.1 M ; $[Fe(III)]_0$ = 1 mM ; $[TiO_2]$ = 1.0 g/L ; $[4\text{-Chlorophenol}]_0$ = $[\text{Benzoic acid}]_0$ = 1 mM ; pH_0 = 1.8 ; N_2 gas purging ; [Xenon lamp : 150 W] ; [Reaction time : 40 min]
WE = Platinum plate (2.5 cm X 1.5 cm) ; CE = Platinum plate ; RE = Calomel electrode ;
Bias potential = +0.7 V

In Figure 40, as revealed by photocurrent electrodes analysis when material was under dispersion condition, it reports a definite mechanism for the visible light responses in the aqueous photo-oxidation on cobalt doped H_2O_2-TiO_2. As shown in Figure 40, it shows the photocurrent voltage characteristics under different target compound conditions (Venkatachalam *et al.*, 2013). As mentioned upper, cobalt doped H_2O_2-TiO_2 could not decompose benzoic acid, but it could degrade 4-chlorophenol very well such as Figure 35. When some target was 4-chlorophenol, the electrons of this material formed aggressive electro-flow. It implies that the electrons on the surface of cobalt doped H_2O_2-TiO_2 were activated by contacting the target compounds such as 4-chlorophenol, which could be degraded very well. It could move into target with the stream. In other words, the moved electrons

mean 'the well-spent electrons'. So, due to the consumed electrons, we can guess that cobalt doped H_2O_2-TiO_2 could not have the good reusability of the efficiency as some fatal photocatalysts.

Finally, we propose the following possible mechanism for cobalt doped H_2O_2-TiO_2. In this study, we have additionally tried to certify the mechanism of visible light response of cobalt doped nanomaterial. Actually, there were lots of summations that emphasized on the mechanism of metal doped TiO_2 involved cobalt. So, our theory can be easily explained by the basis on the previous studies of people in the same field.

First of all, if introducing the specific and possible pathway involved in electron-hole pairs, it should be on the basis of the mentioned characterization and experiment data for comparison to efficiency in Figure 40 (Sood *et al*., 2015). In the existence of cobalt doped H_2O_2-TiO_2, the visible light photon could excite some electrons to the conduction band from the valence band on the photocatalyst. Then, the activated electrons might be migrated to the excited band of cobalt doped H_2O_2-TiO_2. The electrons on the conduction band are subsequently transported to the adsorbed oxygen on the material surface directly and it is possible to pass through the doped cobalt. Actually, the doped cobalt ions could pretend to trap more electrons effectively ($Co^{3+} + e_{cb}^- \rightarrow Co^{2+}$) rather than the adsorbed oxygen or other elements. The far more efficient delivery and hindrance of the hole-electrons recombination on the excited band could produce a lot of mobile holes in the valence band. In addition, it is true that the hole on the ground band (E_0 = +2.96 V) is the stronger oxidants than hydroxyl radical (E_0 = +2.76 V) and superoxide anion (E_0 = +0.56 V) could be migrated into cobalt doped H_2O_2-TiO_2 surface owing to the effect of cobalt ions as the metal ions. Especially, in that case of the holes, it would be charge of greater mineralization of 4-chlorophenol target compound (h_{vb}^+ + 4-CP $\rightarrow$ CO_2 + H_2O) with superoxide radical effects regarding cobalt doped H_2O_2-TiO_2. This is supported with photocurrent and many other data. Then, to rejuvenate the photocatalytic response, the hole on the valence band could oxidize the electrons on the excited band ($h_{vb}^+ + Co^{2+} \rightarrow Co^{3+}$). The photocatalytic flow by the internal cobalt ions could continue until the visible light might be irradiated to cobalt doped H_2O_2-TiO_2 photocatalyst. The explanation could develop the charge separation ability. Also, it was possible to influence on enhancement of the oxidation by the photo-generated hole to decompose the target compounds. Plus, the additional factors such as surface area and the crystallization reported that non-compensated nature of unfair charge state could ensure the formation of flexuous intermediate band, which could effectively close the band gap and estimate that it has the effective electron-hole pair separation under visible light area (400 - 780 nm). In conclusion, it could be the additionally logical basis in regard with the advanced visible light photoactivity of cobalt doped H_2O_2-TiO_2.

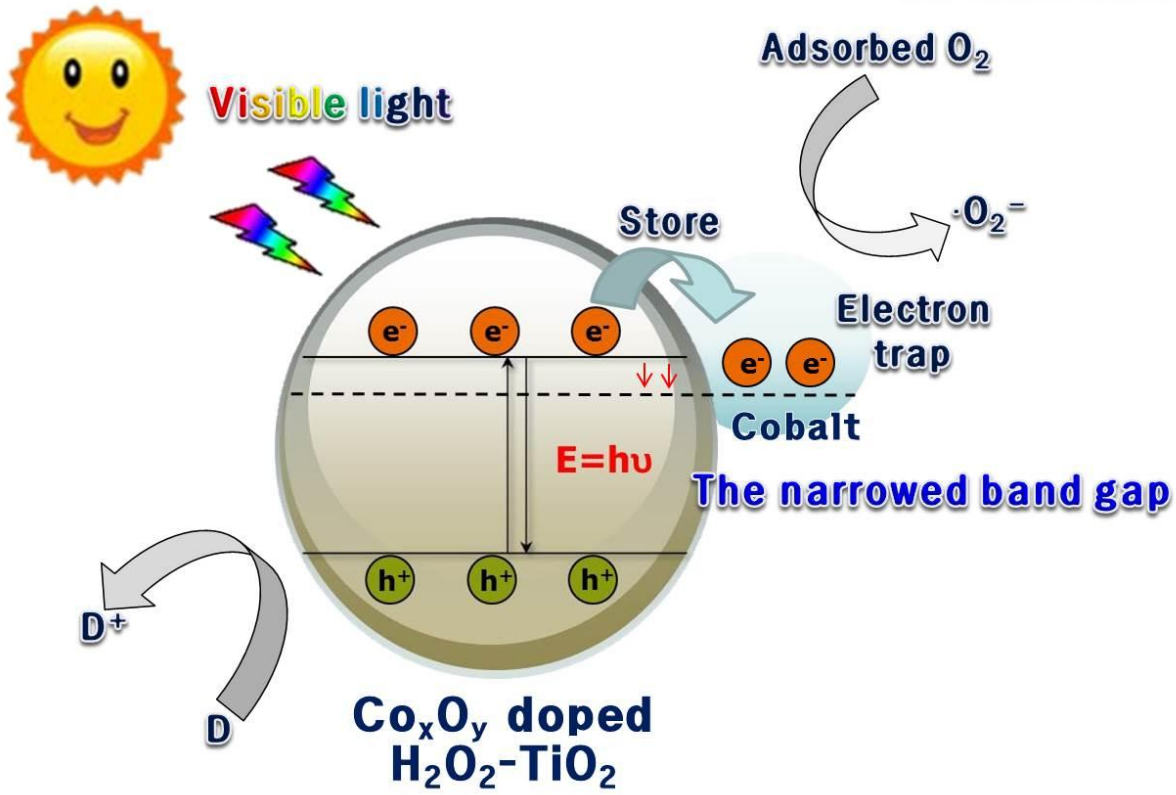

Figure 41. Diagram for demonstrating a mechanism of Co-H_2O_2-TiO_2 in regard with the effect of the metal doping

Chapter 4. Conclusions

The first part of this study was investigated nitrogen doped titanium dioxide by 2-ethylimidazole. N-doped TiO_2 could demonstrate the photocatalytic response under visible light condition (Asahi *et al*., 2001). These were excellently fulfilled through a modified calcination method by using 2-ethylimidazole as nitrogen sources (Burda *et al*., 2003). This was also used to decompose microcystin-LR and to evaluate among other N-doped TiO_2. 2-ethylimidazole-TiO_2 has better photocatalytic response than bare photocatalyst and other nitrogen doped TiO_2 under visible light irradiation. In our study, different N-doped photocatalysts was compared with 2-ethylimidazole-TiO_2 by photocatalytic efficiencies of TiO_2 during 4-chlorophenol degradation time in visible light response abilities. Additionally, XPS data shows that the special binding energy peaks of N 1s were around 400 eV. It implied that the nitrogen was involved on the inside structure of the photocatalyst. Among three N-doped photocatalysts for the comparison of all efficiencies, 2-ethylimidazole-TiO_2 showed the best N-doped TiO_2 with the greatest visible light absorption capacity and effectiveness in 4-chlorophenol and microcystin-LR degradation. The result of the kinetic study was described as the photocatalytic procedures complied with the pseudo-first-order reaction and rate constant. The 4-chlorophenol and microcystin-LR mineralization of entire N-doped TiO_2 could be arranged in the following order: 2-ethylimidazole-TiO_2 > N-doped TiO_2 (Ananpattarachai *et al*., 2009) > N-doped TiO_2 (Kim *et al*., 2014) > N-doped TiO_2 (Choi *et al*., 2007) > bare TiO_2 (Degussa P25). Among three N-doped TiO_2, 2-ethylimidazole-TiO_2 certainly showed the best photocatalytic response when comparing with the remained N-doped photocatalysts. In addition, XRD and TEM data explained that the crystallization of 2-ethylimidazole-TiO_2 was almost same with bare TiO_2 (P25) and XPS analysis implied that the nitrogen replaced the O in the formation of Ti-O-N. The decomposition of target compounds using 2-ethylimidazole-TiO_2 was found to be satisfactory under visible light condition.

The second part of this study developed previous study in regard with H_2O_2-TiO_2. The cobalt doped H_2O_2-TiO_2 material was fabricated by the facile steps and doped as newly visible light response photocatalyst, which could supplement the weak reusability of H_2O_2-TiO_2. As a result, Co-H_2O_2-TiO_2 was successfully fabricated by the sol-gel method for metal doping. This new photocatalysts system, Co-H_2O_2-TiO_2, demonstrated high photoactivity in regard with degradation of 4-chlorophenol as compared with H_2O_2-TiO_2 and the bare TiO_2 (P25) photocatalysts under visible light irradiation condition. Also, Co-H_2O_2-TiO_2 nanoparticles take a tiny size. Therefore, it could have the larger surface areas and visible light activity. Through mentioned analysis, it was proved that the appropriate doping concentration of cobalt ions into TiO_2 matrix derives to the controlled recombination of holes and electrons charge carrier (Kim *et al*., 2005). Thereby, it was estimated at improving photochemical quantum efficiency. Enhancement in photoactivity of Co-H_2O_2-TiO_2 is entirely owing to the important

role of the internal cobalt ions, which could improve the superficial area, make the better visible light response capacity, and prolong the recombination time of the electron-hole pairs. In addition, the leverages of cobalt dopant in regard with photocatalytic behavior of TiO_2 nanoparticles were decisively tried. Plus, the maximum decomposition rate of 4-chlorophenol was perfectly well appreciated in 1 h when the cobalt nitrate concentration was 0.2 mM without any disturbance. Eventually, this study could be proposed as the facile and promising operation in regard with the specific field of the chemical engineering and environment purification project with energy conservation. Finally, we eagerly look forward to providing some useful strategies and new visible light response photocatalyst derived by the chemical methods for doping.

REFERENCES

Fujishima, A., Honada, K. (1972). Photolysis-decomposition of water at the surface of an irradiated semiconductor. *Nature*, 238(5358), 37-38.

Cho, M., Chung, H., Choi, W., & Yoon, J. (2005). Different inactivation behavious of MS-2 phage and Eschericha coli in TiO_2 photocatalytic disinfection. *Appl. Environ. Microbiol*, 71(1), 270-275.

Gerischer, H., & Heller, A. (1992). Photocatalytic oxidation of organic molecules at TiO_2 particles by sunlight in aerated water. *J.Electrochem. Soc*, 139(1), 113-118.

Reyes-Coronado, D., Rodriguez-Gattorno, G., Espinosa-Pesqueira M. E., Cab C., Coss, R. de., & G Oskamo (2008). Phase-pure TiO_2 nanoparticles: anatase, brookite and rutile. *Nanotechnology*, 19(14).

Hoffmann, M. R., Martin, S. T., Choi, W., & Bahnemann, D. W. (1995). Environmental applications of semiconductor photocatalysis. *Chem.Rev.*, 95(1), 69-96.

Linsebigler, A. L., Lu, G., & Yates Jr, J. T. Photocatalysis on TiO_2 surface: principle , mechanisms, and selected results. *Chem.Rev.*, 95(3), 735-758.

Wu, T., Liu, G., & Zhao, J. (1999). Evidence for H_2O_2 generation during the TiO_2-assisted photodegradation of dyes in aqueous dispersions under visible light illumination. *J. Phys. Chem. B*, 103(23), 4862-4867.

Wang, C., Pagel, R., Bahnemann, D. W., & Dohrmann, J. K. (2004). Quantum yield of formaldehyde formation in the presence of colloidal TiO_2-based photocatalysts: Effect of intermittent illumination, platinization, and deoxygenation. . *J. Phys. Chem. B*, 108(37), 14082-14092.

Bacsa, R., Kiwi, J., Ohno, T., Albers, P., & Nadtochenko, V. (2005). Preparation, testing and characterization of doped TiO_2 active in the peroxidation of biomolecules under visible light. *J. Phys. Chem. B*, 109(12), 5994-6003.

Wang, J., Tafen, D. N., Lewis, J. P., Hong, Z., Manivannan, A., Zhi, M., Li, M., & Wu, N. (2009). Origin of photocatalytic activity of nitrogen-doped TiO_2 nanobelts. *J. Am. Chem. Soc*, 131(34), 12290-12297.

Ohno, T., Mitsui, T., & Matsumura, M. (2003). Photocatalytic activity of S-doped TiO_2 photocatalyst under visible light. *Chemistry Letters*, 32(4), 364-365.

Sathish, M., Viswanathan, B., Viswanath, R. P., & Gopinath, C. S. (2005). Synthesis, characterization, electronic structure, and photocatalytic activity of nitrogen-doped TiO_2 nanocatalyst. *Chem. Mate*, 17(25), 6349-6353.

Morikawa, T., Asahi, T., Ohwaki, T., Aoki, K., & Taga, Y. (1992). Band-gap narrowing of titanium dioxide by nitrogen doping. *Japanese Journal of Applied Physics*, 40(2), 6A.

Jagadale, T. C., Takale, S. P., Sonawane, R. S., Joshi, H. M., Patil, S. I., Kale, B. B., & Ogale, S. B. (2008). N-doped TiO_2 nanoparticle based visible light photocatalyst by modified peroxide sol-gel method. *J. Phys. Chem. C*, 112(37), 14595-14602

Choi, H., Antoniou, M. G., Pelaez, M., Armah A. De La Cruz, Shoemaker, J. A., & Dionysiou, D. D. (2007). Mesoporous nitrogen-doped TiO_2 for the photocatalytic destruction of the cyanobacterial toxin microcystin-LR under visible light irradiation. *Environ. Sci. Technol*, 41(21), 7530-7535.

Kim, W., Tachikawa, T., Kim, H., Lakshminarasimhan, N., Murugan, P., Park, H., Majima, T., & Choi, W. (2014). Visible light photocatalytic activities of nitrogen and platinum-doped TiO_2: synergistic effects of co-dopants. *Applied Catalysis B: Environmental*, 147, 642-650.

Ananpattarachai, J., Kajitvichyanukul, P., & Seraphin, S. (2009). Visible light absorption ability and photocatalytic oxidation activity of various interstitial N-doped TiO_2 prepared from different nitrogen dopants. *Journal of Hazardous Materials*, 168, 253-261.

Bubacz, K., Kusiak-Nejman, E., Tryba B., & Morawski, A. W. Investigation of OH radicals formation on the surface of TiO_2/N photocatalyst at the presence of terephthalic acid solution. Estimation of optimal conditions. *Journal of photochemistry and Photobiology A: Chemistry*, 261, 7-11.

Choi, W., Termin, A., & Hoffmann, M. R. The role of metal ion dopants in quantum-sized TiO_2: Correlation between photoreactivity and charge carrier recombination dynamics. (1994). *J. Phys. Chem.*. 98(51), 13669-13679.

Yang, T., Yang, M., Shiu, C., Chang, W., & Wong, M. (2006). Effect of N_2 ion flux on the photocatalysis of nitrogen-doped titanium oxide films by electron-beam evaporation. *Applied Surface Science*, 252(10), 3729-3736.

Hamal, D. B., & Klabunde, K. J. (2011). Valence state and catalytic role of Cobalt ions in Cobalt TiO_2 nanoparticle photocatalysts for acetaldehyde degradation under visible light. *J. Phys. Chem. C*, 115(35), 17359-17367.

Choi, J., Park, H., & Hoffmann, M. R. (2010). Effects of single metal-ion doping on the visible-light photoreactivity of TiO_2. *J. Phys. Chem. C*, 114(2), 783-792.

Tachikawa, T., Tojo, S., Kawai, K., Endo, M., Fujitsuka, M., Ohno, T., Nishijima, K., Miyamoto, Z., & Majima, T. (2004). Photocatalytic oxidation reactivity of holes in the Sulfur- and Carbon-doped TiO_2 powders studied by time-resolved diffuse reflectance spectroscopy. *J. Phys. Chem. B*, 108(50), 19299-19306.

Ohno, T., Masaki, Y., Hirayama, S., & Matsumura, M. (2001). TiO_2-photocatalyzed epoxidation of 1-Decene by H_2O_2 under visible light. *Journal of Catalysis*, *204*(1), 163-168.

Bingham, S., & Daoud, W. A. (2011). Recent advances in making nano-sized TiO_2 visible-light active through rare-earth metal doping. *Joutnal of Materials chemistry*, 21, 2041-2050.

Pettibone, J. M., Cwiertny, d. M., Scherer, M., & Grassian, V. H. (2008Adsorption of organic acids on TiO_2 nanoparticles: Effects of pH, nanoparticle size, and nanoparticle aggregation. *Langmuir*, 24(13), 6659-6667.

Santrucek & Krepelka (1988). Antioxidants-potential chemotherapeutic agents. *Drugs Future*, 13(11), 974-996.

Petrone, W. F., English, D. K., Wong, K., & McCord, J. M. (1980). Free radicals and inflammation: superoxide-dependent activation of a neutrophil chemotactic factor in plasma. *National Acad Sciences*, 77(2), 1159-1163.

Oyanagui, Y. (1982). Macrophage-generated superoxide radicals: Inflammation and tumor cell growth. *Pathology of Oxygen,Academic Press, New York*, 99-106.

Venkatachalam, S., Hayashi, H., Nanjo, H., & Ebina, T. (2013). Preparation and characterization of nanostructured TiO_2 thin films by hydrothermal and anodization methods. *INTECH Open Access Publisher*.

Sood, S, Umar, A., Mehta, S. K., & Kansal, S. K. (2015). Highly effective Fe-doped TiO_2 nanoparticles photocatalysts for visible-light driven photocatalytic degradation of toxic organic compounds. *Journal of Colloid and Interface Science*, 450, 213-223.

Asahi, R., Morikawa, T., Ohwaki, T., Aok,i K., & Taga, Y. (2001). Visible-light photocatalysis in nitrogen-doped titanium oxides. *Science*, 293(5528), 269-271.

Burda, C., Lou, Y., Chen, X., Samia, A. S., Stout, J., & Gole, J. L. (2003). Enhanced nitrogen doping in TiO_2 nanoparticles. *Nano lett*, 3(8), 1049-1051.

Kim, S., Hwang, S. J. & Choi, W. (2005). Visible light active Platinum-ion-doped TiO_2 photocatalyst. *J. Phys.*

ACKNOWLEDGEMENTS